

The effects of induced magnetic mixing in AGB stars

D. Vescovi & S. Cristallo



INAFA - Osservatorio Astronomico d'Abruzzo

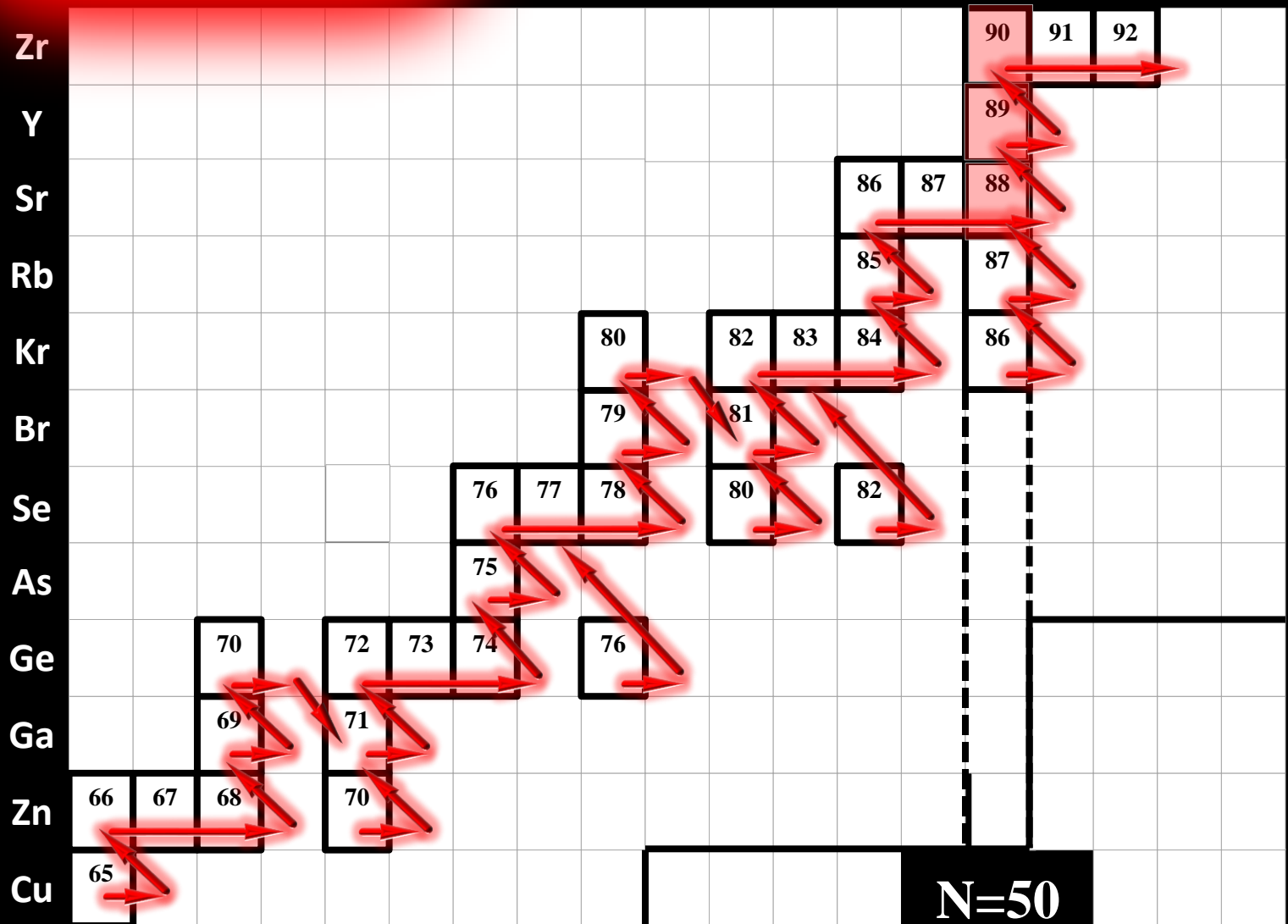
OUTLINE

- PAST: **FRUITY AGB models**
- PRESENT & FUTURE: **Magnetic AGB models**
- Comparison to **observations**:
 1. **Presolar Grains**
 2. **Ba-stars**
 3. **S-stars**
 4. **C-stars**
 5. **Post-AGB stars**

s process

$$N_n \sim 10^7 \text{ n/cm}^3$$

Proton number



N=50

Neutron number

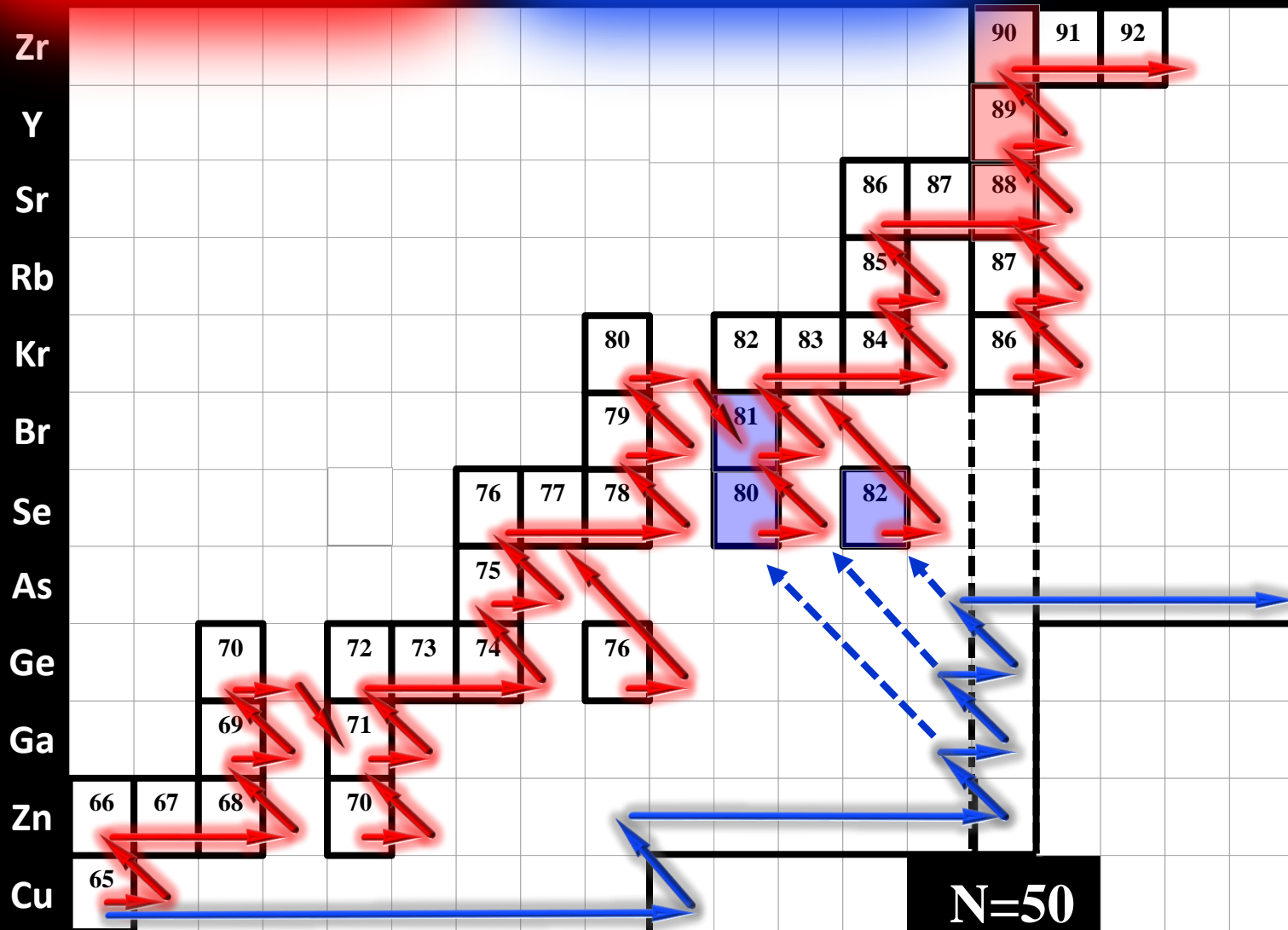
Proton number

s process

$$N_n \sim 10^7 \text{ n/cm}^3$$

r process

$$N_n > 10^{23} \text{ n/cm}^3$$



Neutron number

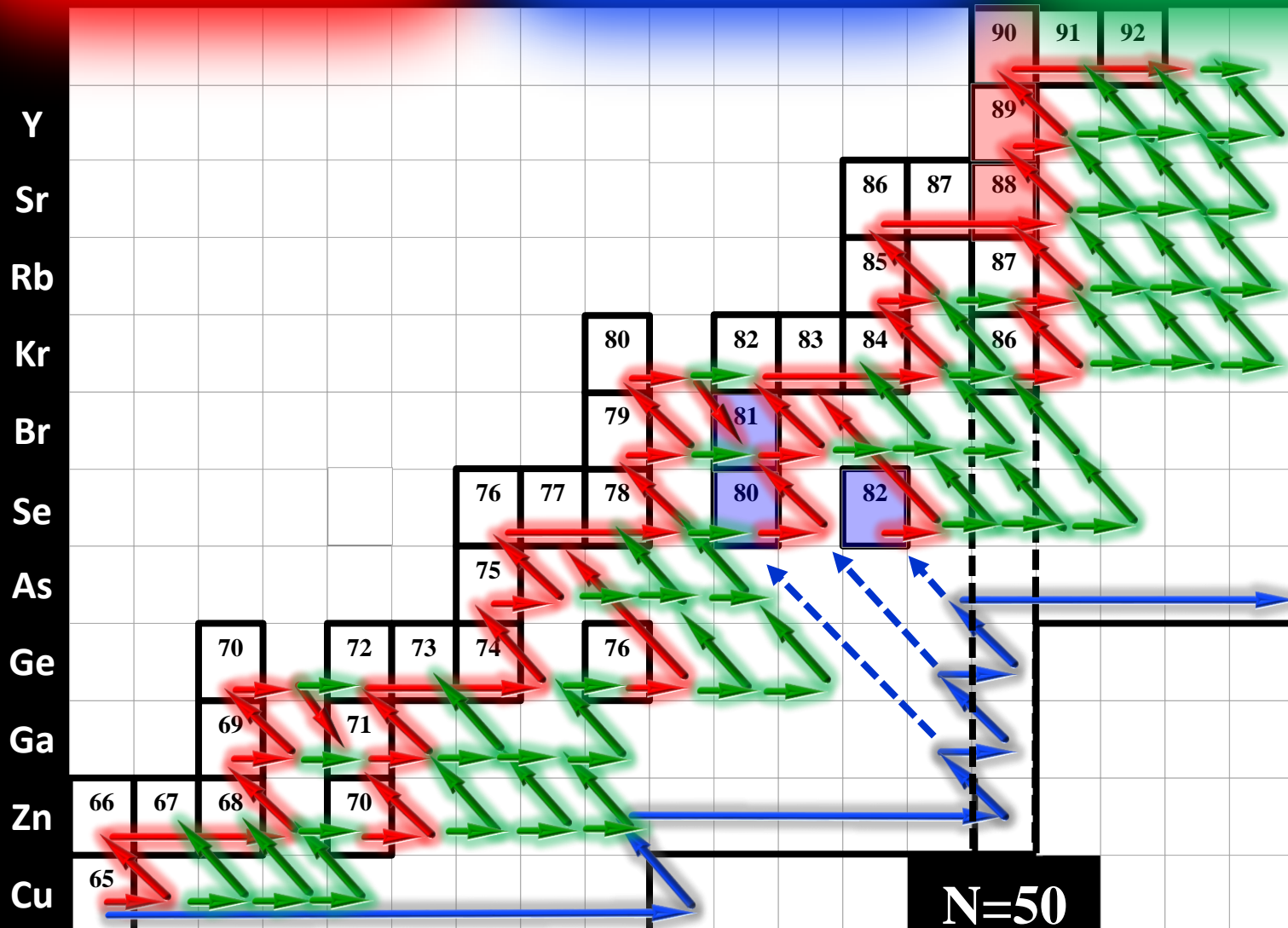
N=50

Proton number

s process
 $N_n \sim 10^7 \text{ n/cm}^3$

r process
 $N_n > 10^{23} \text{ n/cm}^3$

i process
 $N_n \sim 10^{14-17} \text{ n/cm}^3$



Neutron number

N=50

F.R.U.I.T.Y.

FULL-Network Repository of Updated Isotopic Tables & Yields

F.R.U.I.T.Y.
(FULL-Network Repository of Updated Isotopic Tables & Yields)

Select Data:

MODEL SELECTION	OUTPUT SELECTION	OUTPUT FORMAT	
Mass (M_{\odot}) ---	Nuclides Properties <input type="radio"/> Elements ^(3,4) Z: All <input type="radio"/> Isotopes ⁽⁵⁾ A: All Z: All <input type="radio"/> s-process ⁽⁶⁾ : [hs/ls], [Pb/hs], ... <input type="radio"/> Net ⁽⁸⁾ Yields ⁽⁷⁾ A: All Z: All <input type="radio"/> Total	Multiple Table format ⁽¹⁰⁾	Single Table format ⁽¹¹⁾
Metallicity (Z) ⁽¹⁾ ---		<input checked="" type="radio"/> All Dredge Up Episodes ⁽¹²⁾	<input type="radio"/> Final Composition
Initial Rotational Velocity (IRV) ⁽²⁾ 0		<input type="radio"/> Final	<input type="radio"/> Final
¹³ C Pocket ⁽⁹⁾ Standard			

[NOTES ON THE MODELS \(pdf file\)](#)

SC+ 2011, 2015

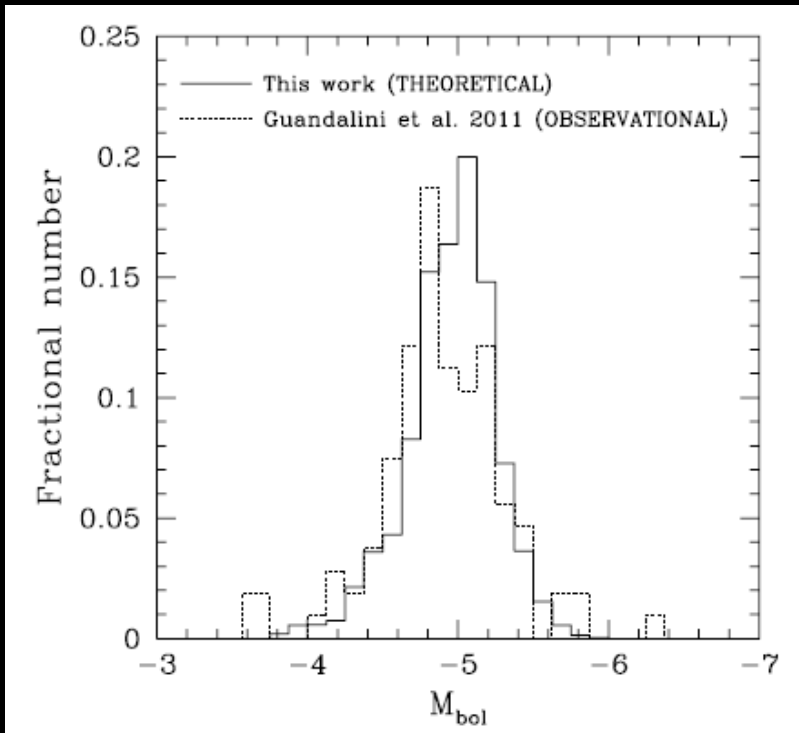
fruity.oa-abruzzo.inaf.it

$-2.85 \leq [\text{Fe}/\text{H}] \leq +0.3$

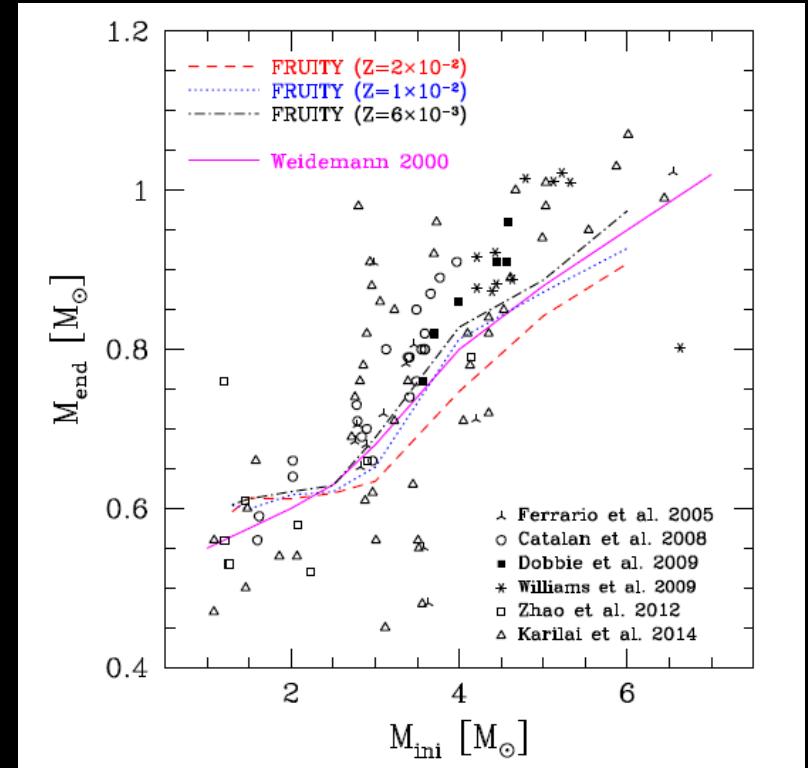
$1.3 \leq M/M_{\text{sun}} \leq 6.0$

OBSERVATIONS (physics)

Luminosity Function of C-stars



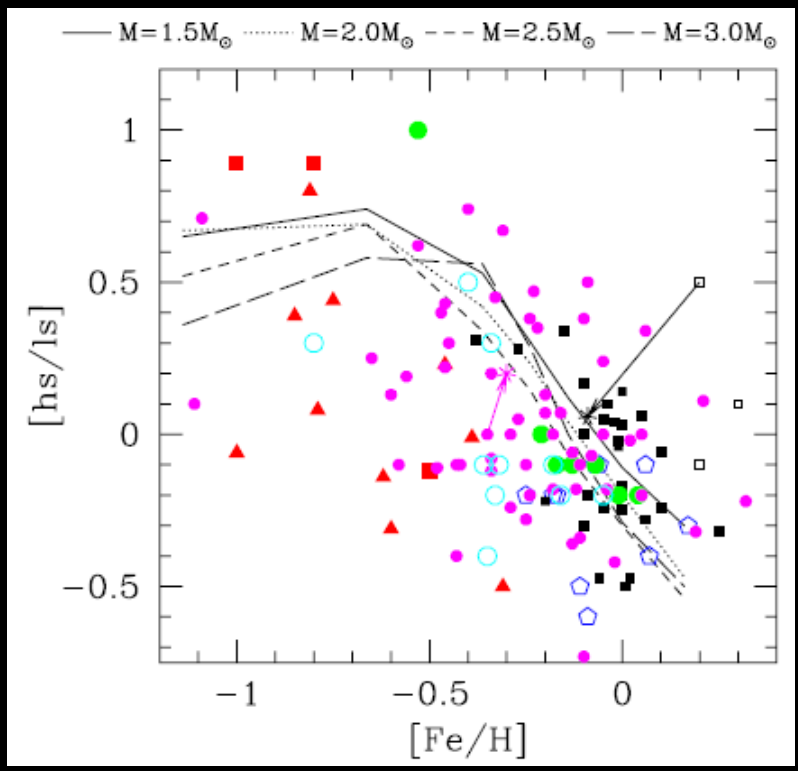
Initial-to-final mass relations



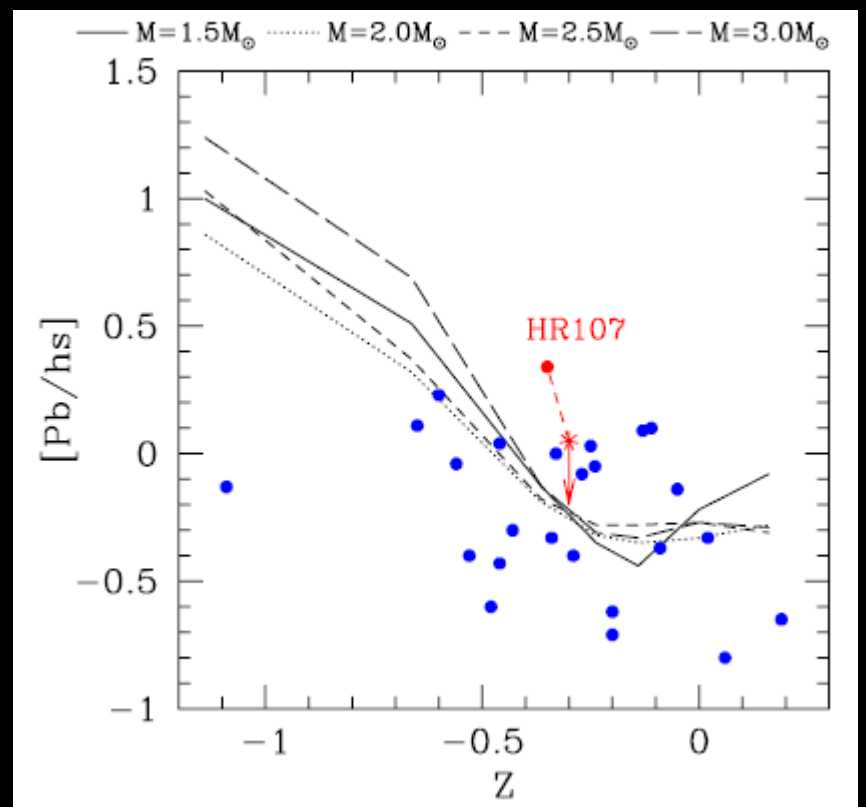
SC+ 2011

OBSERVATIONS (spectroscopy)

Second to first s-process peak



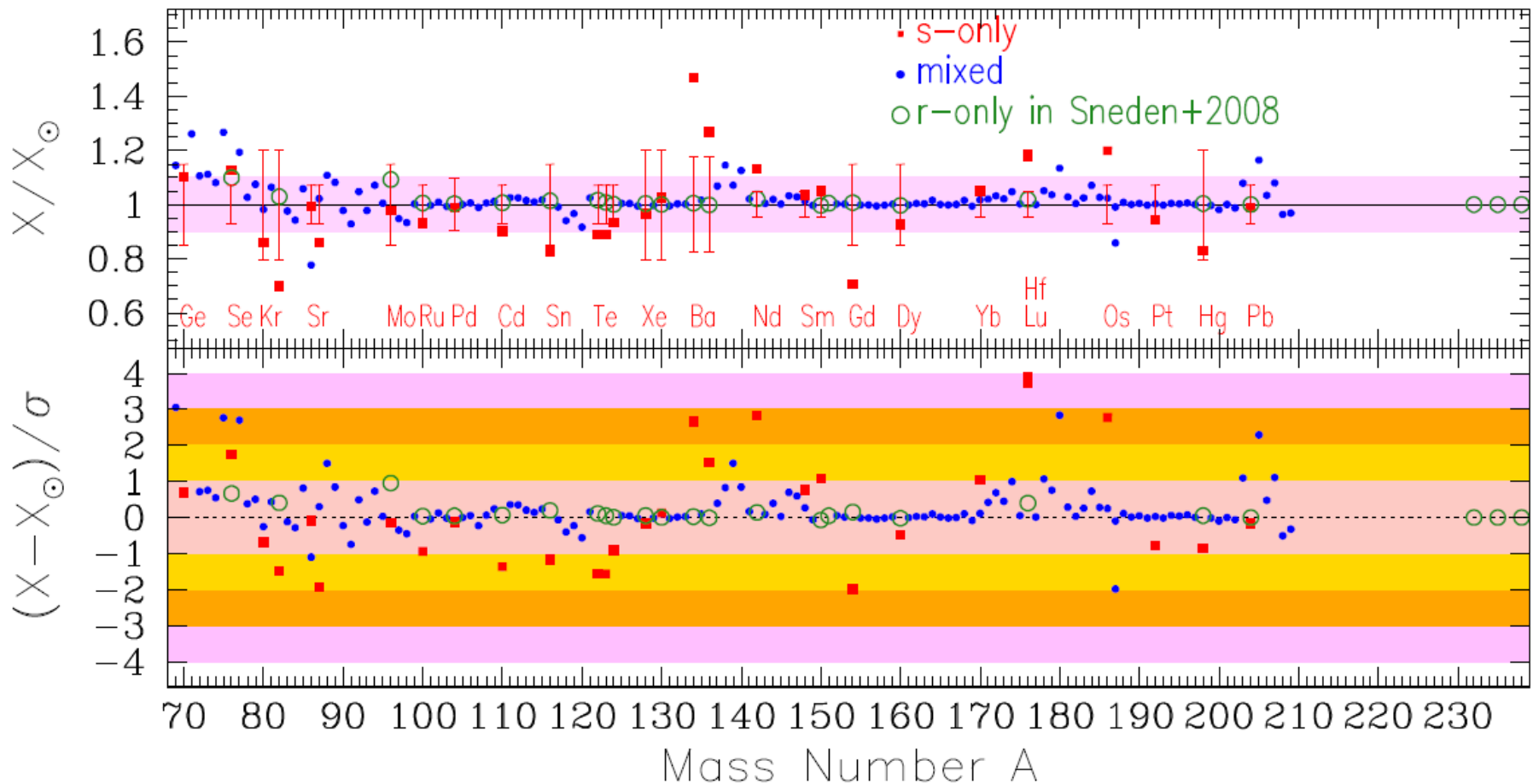
Third to second s-process peak



SC+ 2011

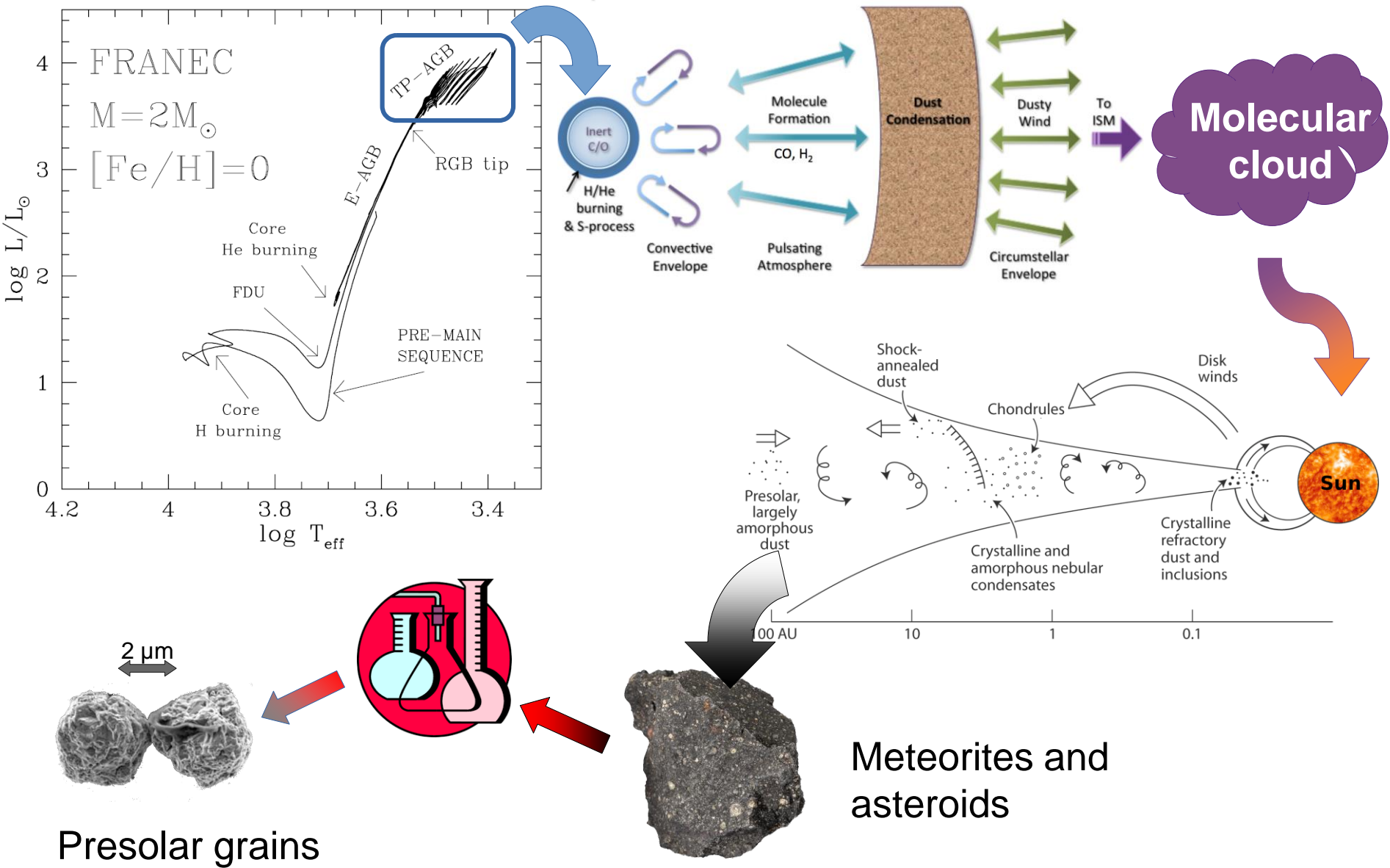
- [ls/Fe] = [Sr, Y, Zr/Fe]
- [hs/Fe] = [Ba, La, Ce, Nd/Fe]
- [hs/ls] = [hs/Fe] - [ls/Fe]

Comparison to solar distribution



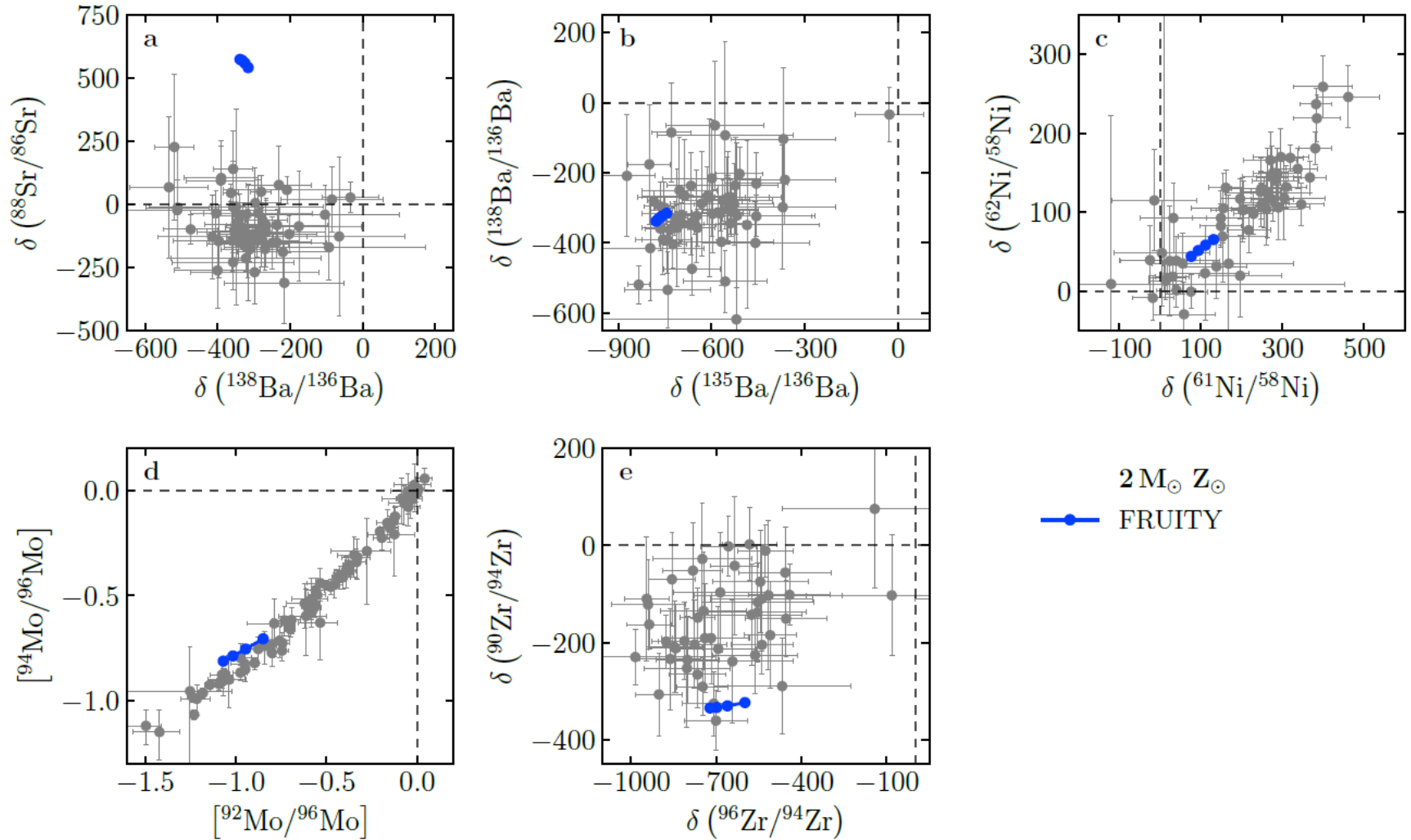
Prantzos+ 2020

AGB stars and presolar SiC grains



SiC Grains

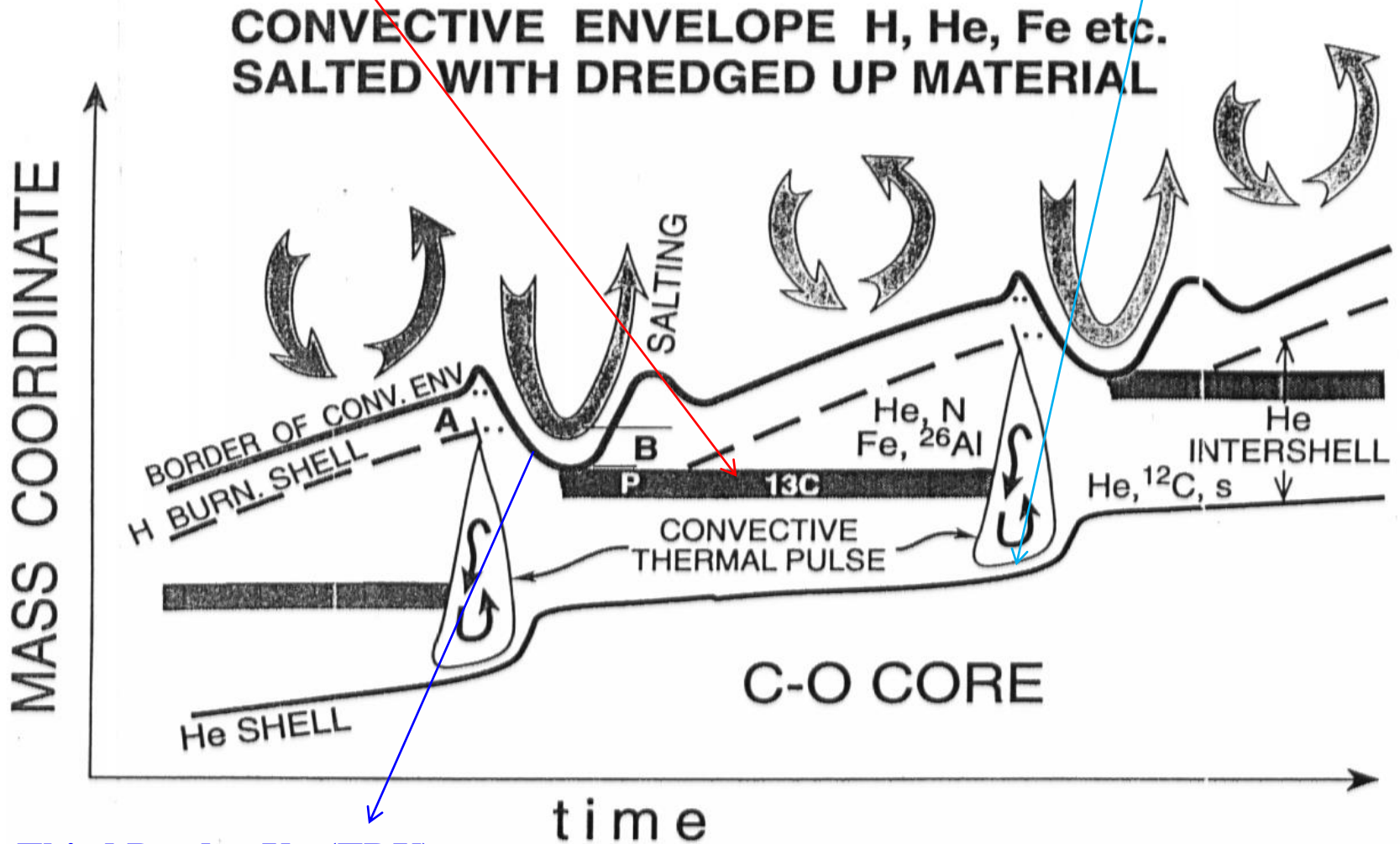
The disagreement between presolar SiC data and models is evident!



The s-process in AGB stars

$^{13}\text{C}(\alpha, n)^{16}\text{O}$ reaction

$^{22}\text{Ne}(\alpha, n)^{25}\text{Mg}$ reaction



Third Dredge Up (TDU)

Busso et al. 1999

The ^{13}C pocket in stellar evolutionary models

- ✓ **Opacity induced overshoot** (SC+2009)
- ✓ **Convective Boundary Mixing + Gravity Waves** (Battino+ 2017)
- ✓ **Magnetic-induced mixing** (Vescovi+2020)

How does the ^{13}C pocket change?

- ✓ **Rotation-induced mixing** (Herwig+ 2003; Siess+ 2004; Piersanti+ 2013)

Our working hypothesis: magnetic induced mixing

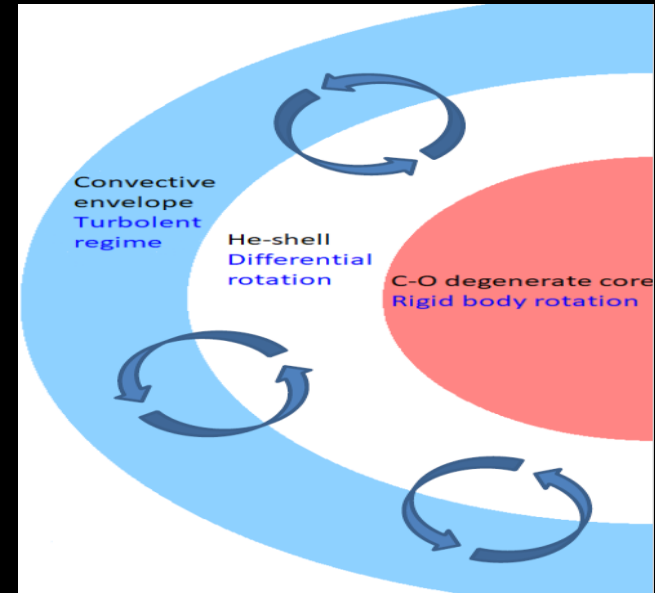
Nucci & Busso 2014

A magnetized stellar plasma in the quasi-ideal MHD regime, with a density distribution closely following a power law as a function of the radius ($r \propto r^k$, with $k < -1$), reaches a dynamic equilibrium and is in radial expansion.

In strong field regimes, the magnetic field tends to concentrate in flux tubes. As a consequence of the magnetic extra-pressure, these tubes are buoyant (see, e.g., Parker 1955).

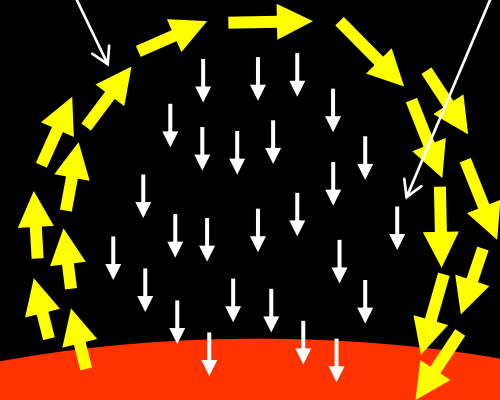
$$p(z) = p_1(z) + B^2/8\pi$$

Due to the effect of the magnetic buoyancy, a matter flow is pushed from the He-intershell to the envelope. This, in turn, induces a downflow flux, in order to guarantee mass conservation.

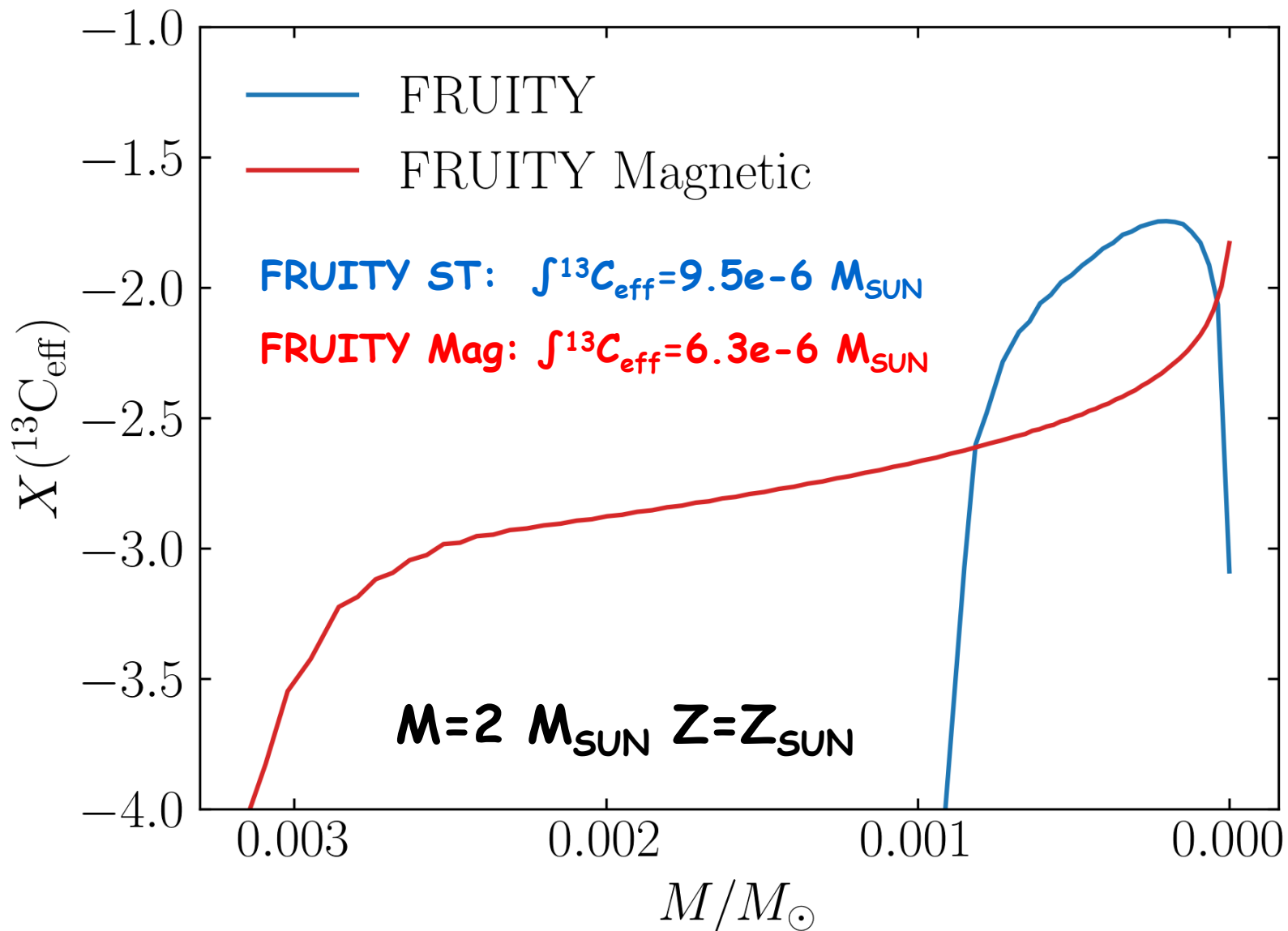


Fast rising magnetized tube

Slow settling non-magnetized material

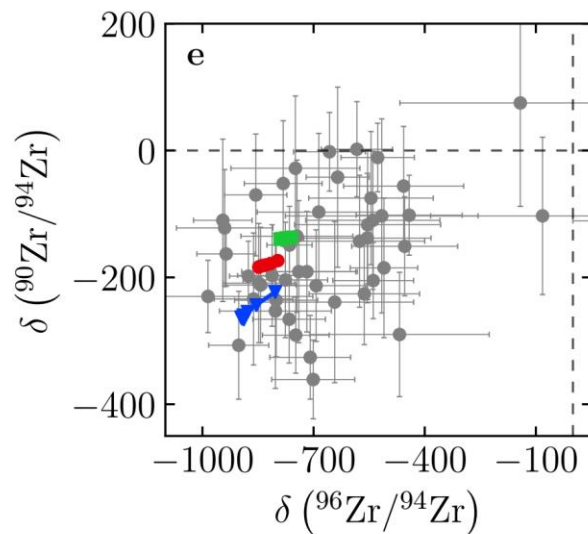
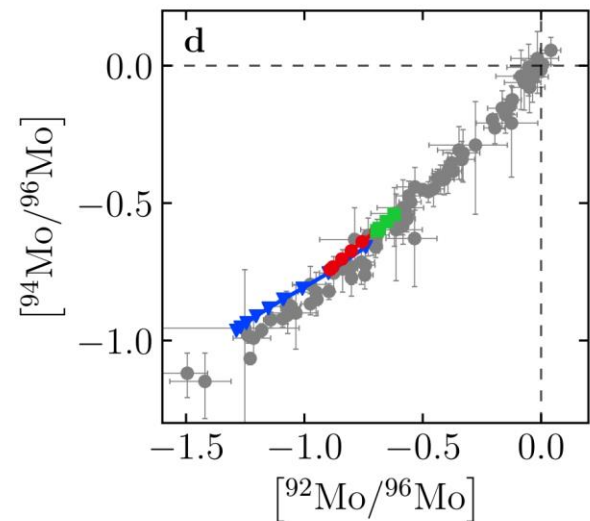
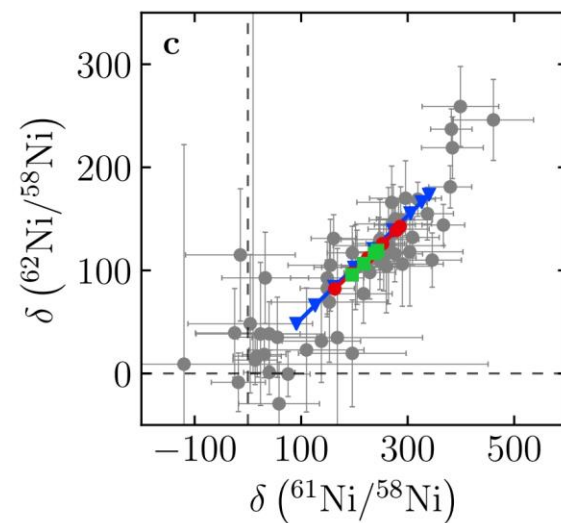
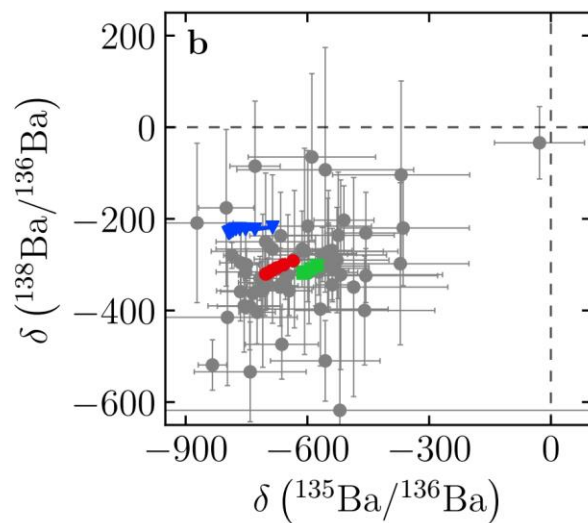
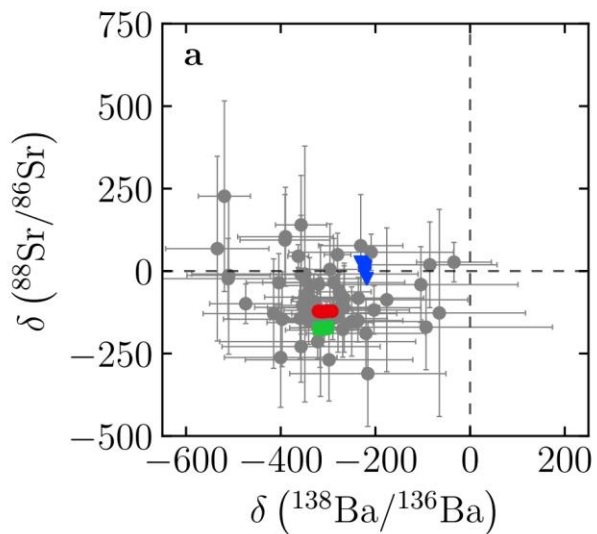


Magnetic ^{13}C -pocket vs FRUITY ^{13}C -pocket



SiC Grains

- **Magnetic** contribution account for SiC data!!
- Best fit for $u_p = 5 \times 10^{-5}$ cm/s and $B_\phi = 5 \times 10^4$ G



2 M_\odot FRUITY Magnetic
— ∇ $Z = 0.01$
— \bullet $Z = Z_\odot$
— \square $Z = 0.02$

Vescovi+ 2020

WHAT'S NEXT?

- **Ba stars (extrinsic AGBs)**
- **C-stars**
- **S-stars**
- **Post-AGB stars**

The origin of magnetic fields in stars

Still largely debated topic:

1. fossil relics in stably stratified radiative regions (inherited from previous evolutionary phases);
2. dynamo-generated in turbulent convective layers.

Since the time-scale for ohmic decay of a large-scale field is typically longer than the star's lifetime, the **radiative regions** may be regarded as perfectly conducting and the magnetic field is then "**frozen**" into the plasma.

During a Thermal Pulse, **turbulence** leads to rapid reconnection that dissipates any large-scale coherent field.

HOWEVER, convection, rotation, and shear within the convective region will regenerate the field through **dynamo action**: numerical simulations suggest that convective layers are site of very efficient small-scale dynamos.

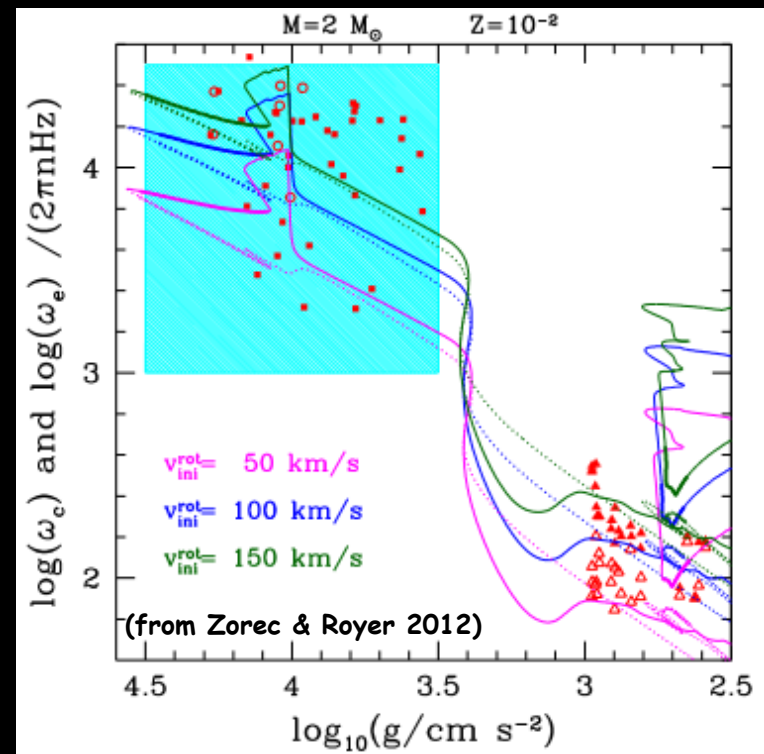
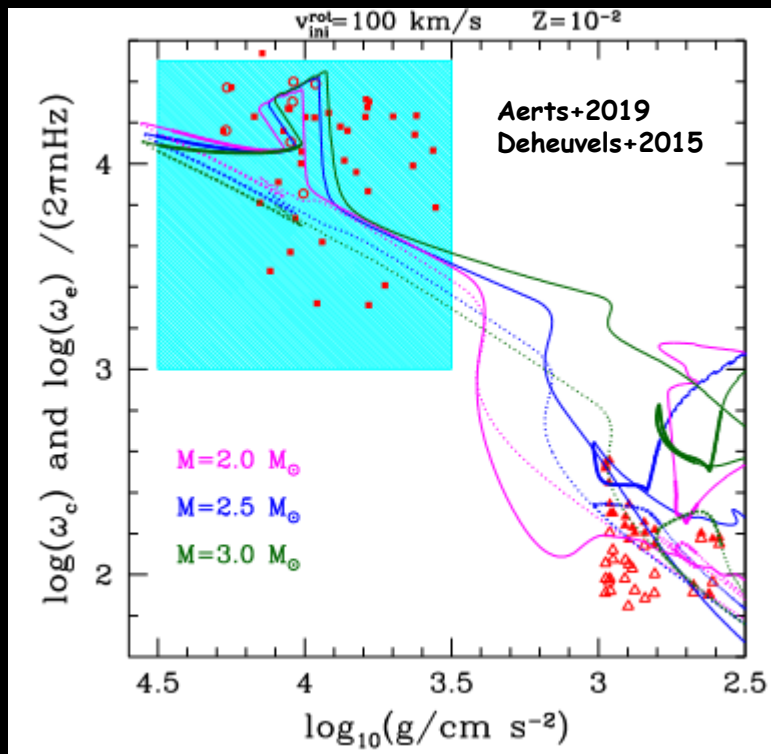
BUT: we are interested in a **axisymmetric toroidal magnetic field**.

The origin of magnetic fields in stars

Such a field could be achieved through the stretching of a preexisting low-magnitude poloidal field in the radiative zone below the convective envelope after the quenching of a thermal pulse, via the action of differential rotation around the rotation axis.

$$B_{\phi} \sim B_p(\Omega q \Delta t) \quad q = \partial \ln \Omega / \partial \ln r$$

$$B_p \approx 5 \text{ G} \rightarrow B_{\phi} \approx 5 \times 10^4 \text{ G}$$



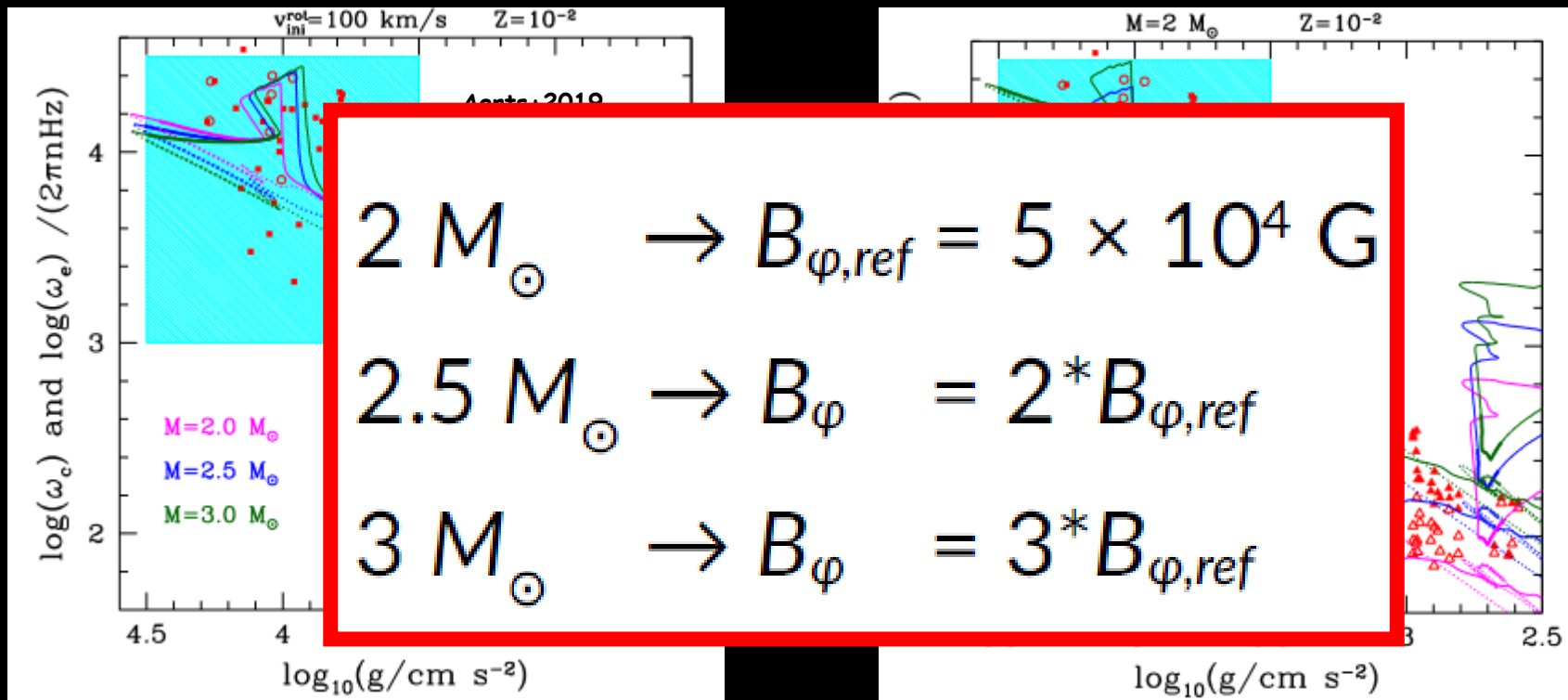
Artificial viscosity added to match asteroseismic data (e.g. **Den Hartogh+2019**).

The origin of magnetic fields in stars

Such a field could be achieved through the stretching of a preexisting low-magnitude poloidal field in the radiative zone below the convective envelope after the quenching of a thermal pulse, via the action of differential rotation around the rotation axis.

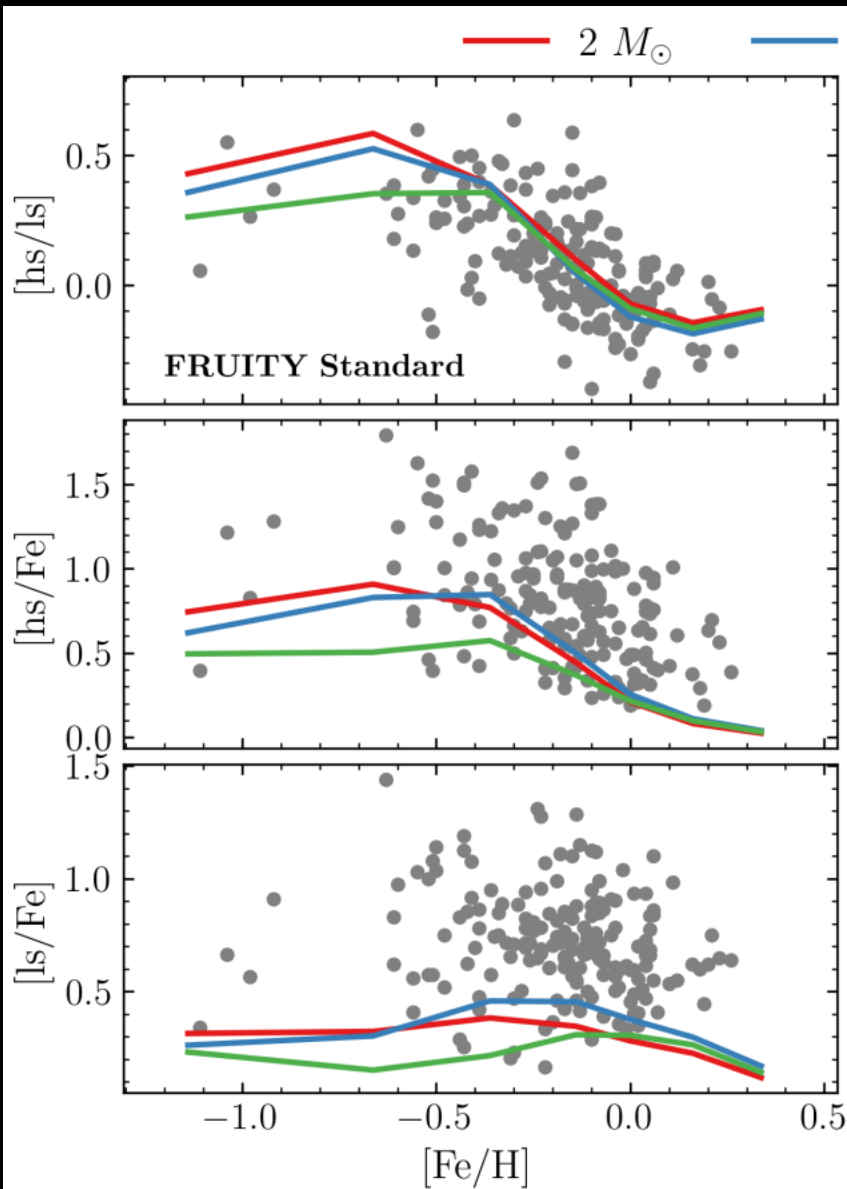
$$B_{\phi} \sim B_p(\Omega q \Delta t) \quad q = \partial \ln \Omega / \partial \ln r$$

$$B_p \approx 5 \text{ G} \rightarrow B_{\phi} \approx 5 \times 10^4 \text{ G}$$



Artificial viscosity added to match asteroseismic data (e.g. **Den Hartogh+2019**).

Ba-stars



Cseh+18

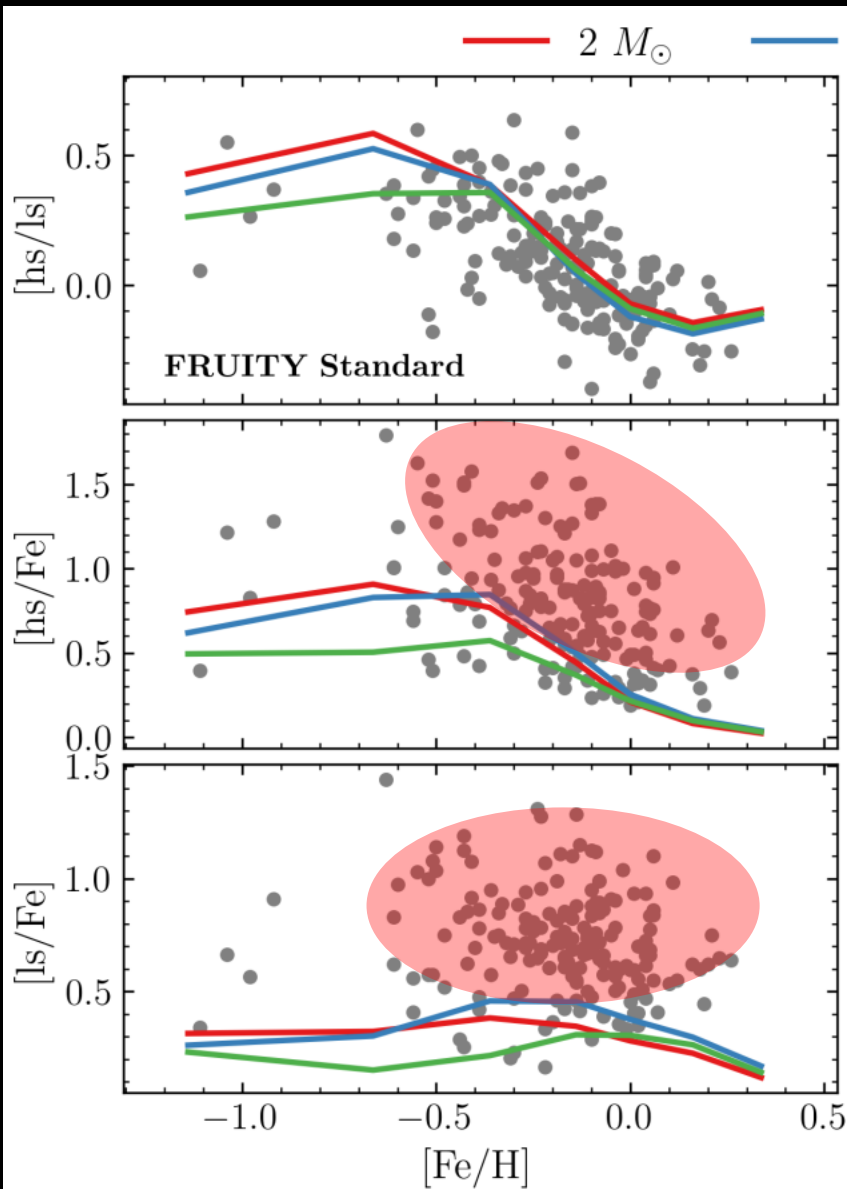
De Castro+16

Pereira+11

Roriz+21a

Roriz+21b

Ba-stars



Cseh+18

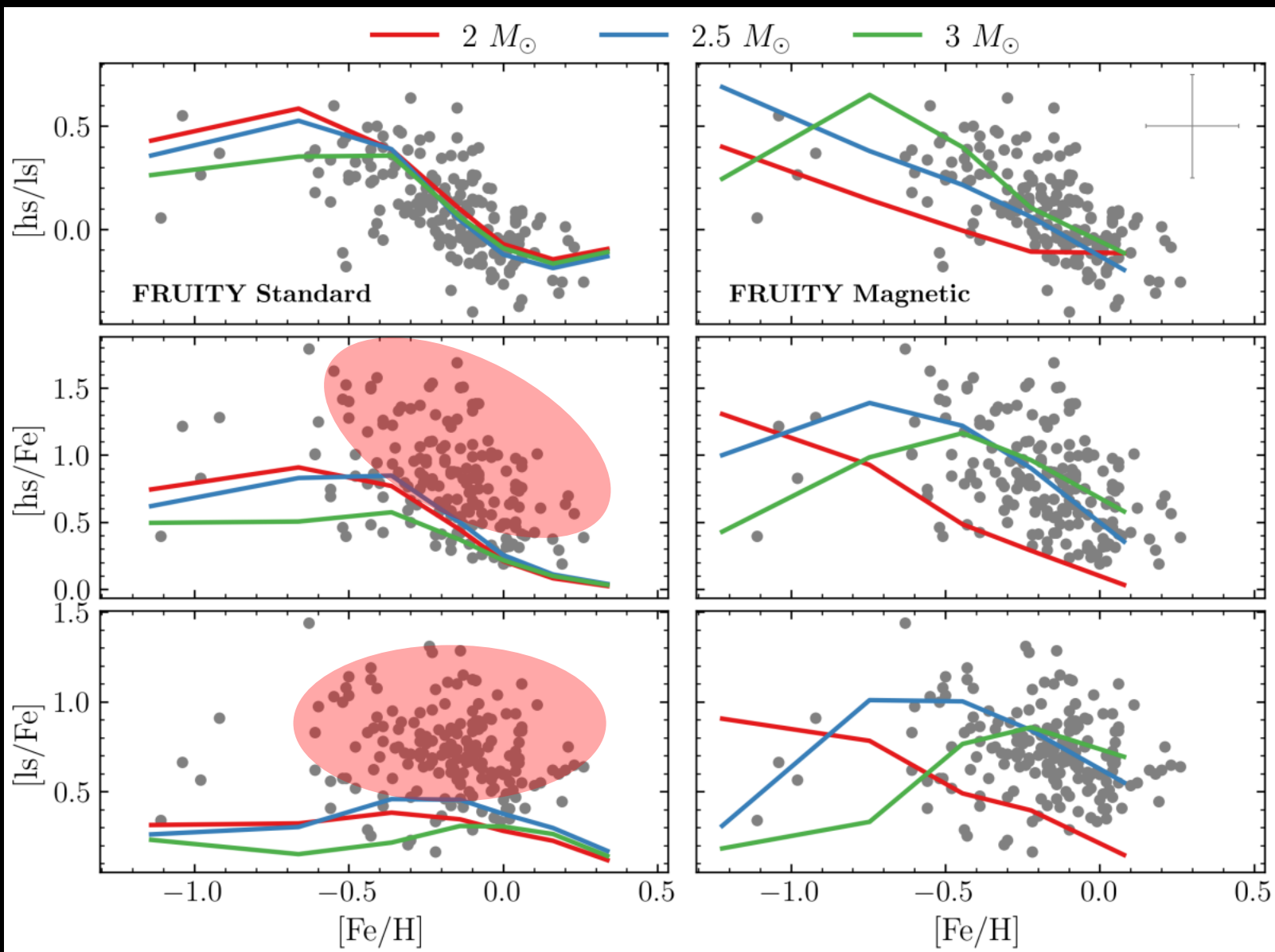
De Castro+16

Pereira+11

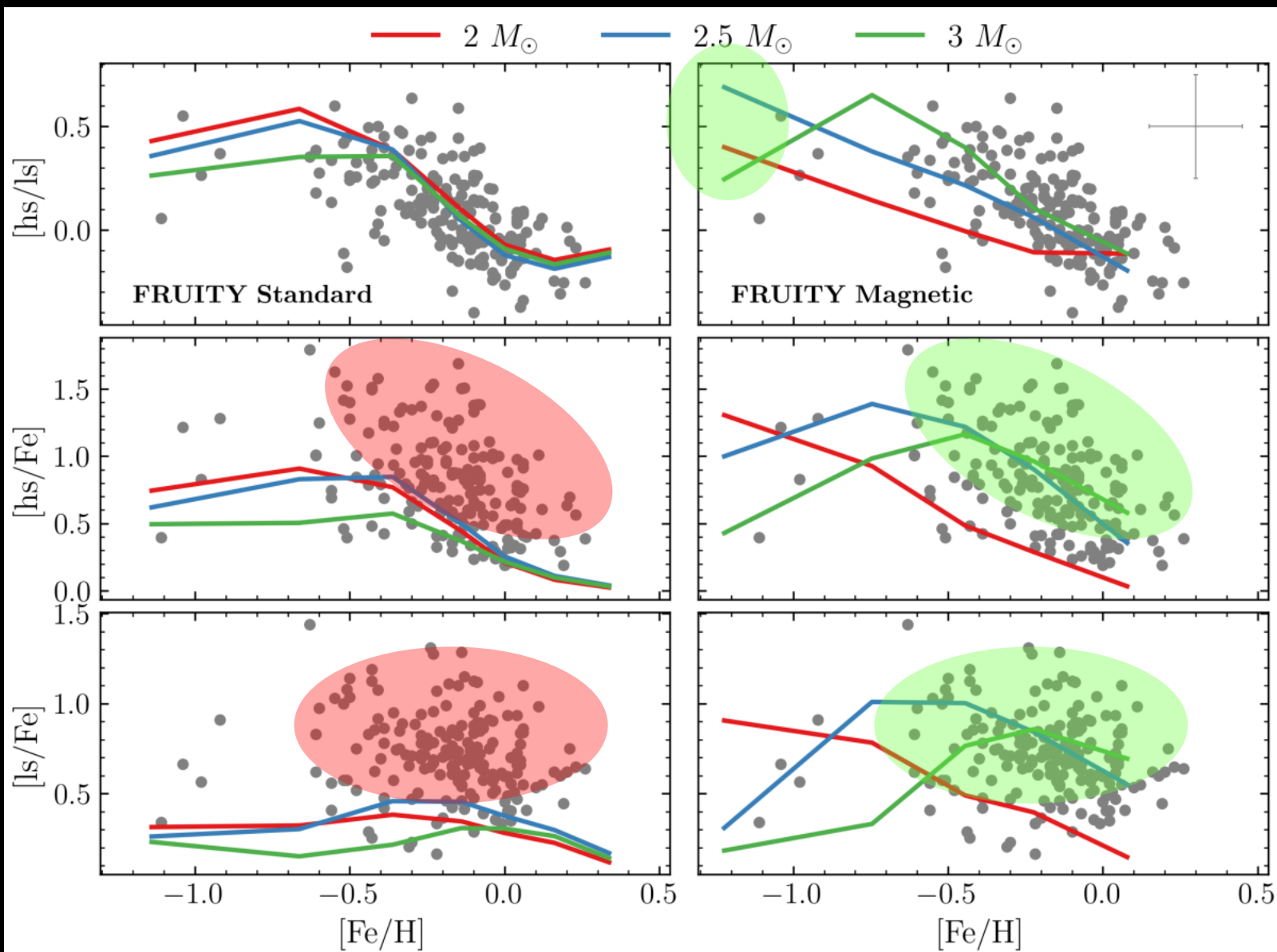
Roriz+21a

Roriz+21b

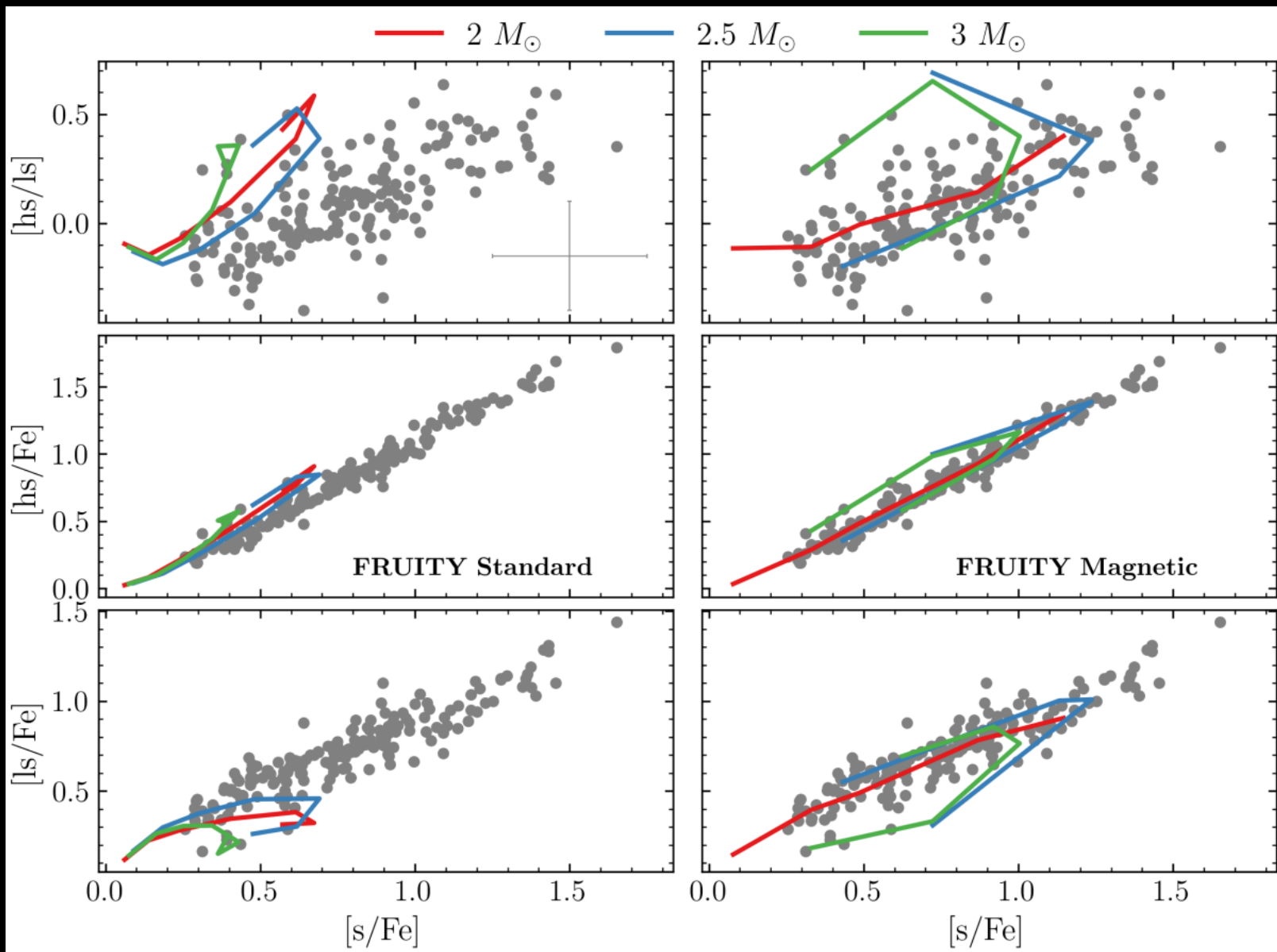
Ba-stars



Ba-stars

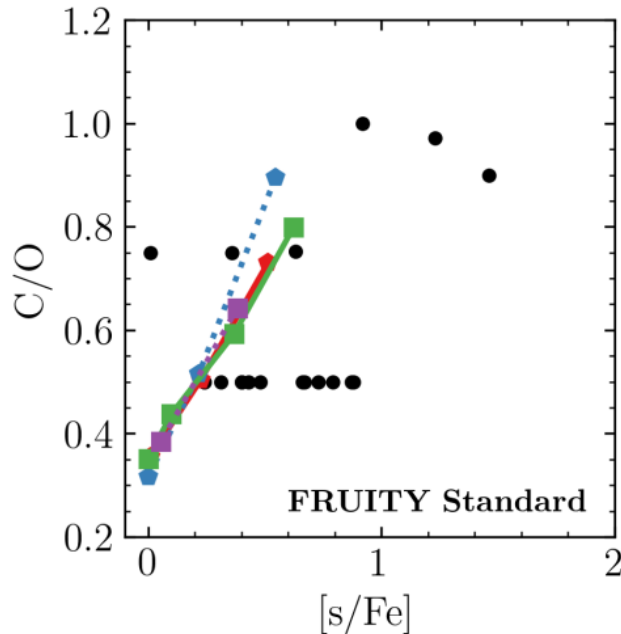
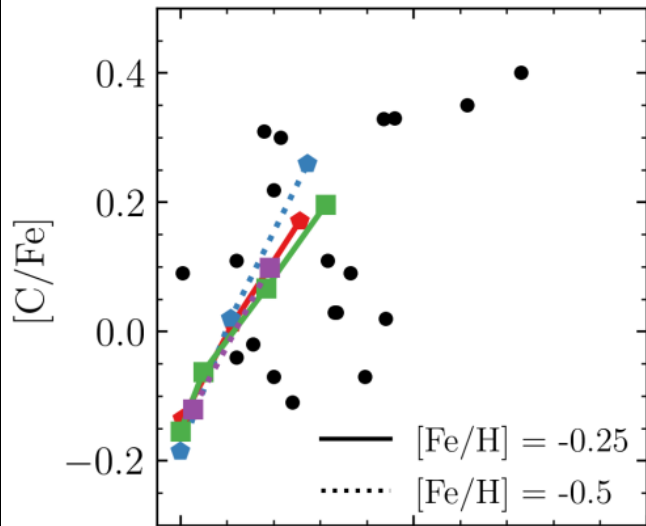


Ba-stars

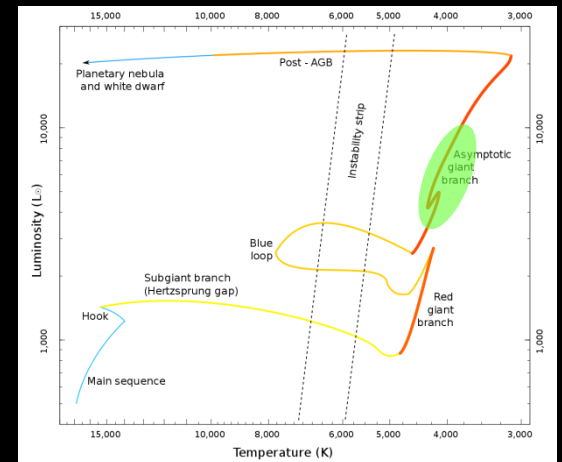


S-stars

$$0.3 < \text{C/O} < 1.0$$

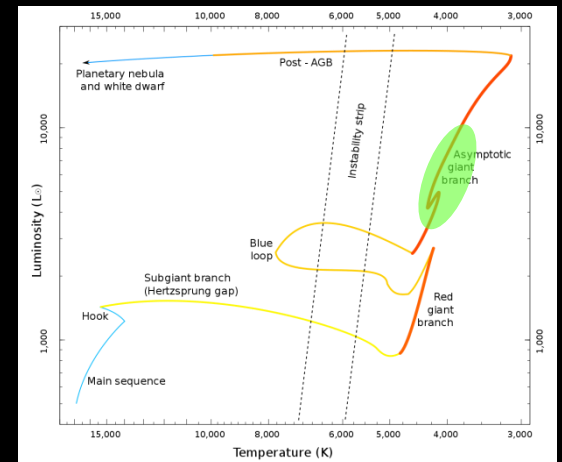
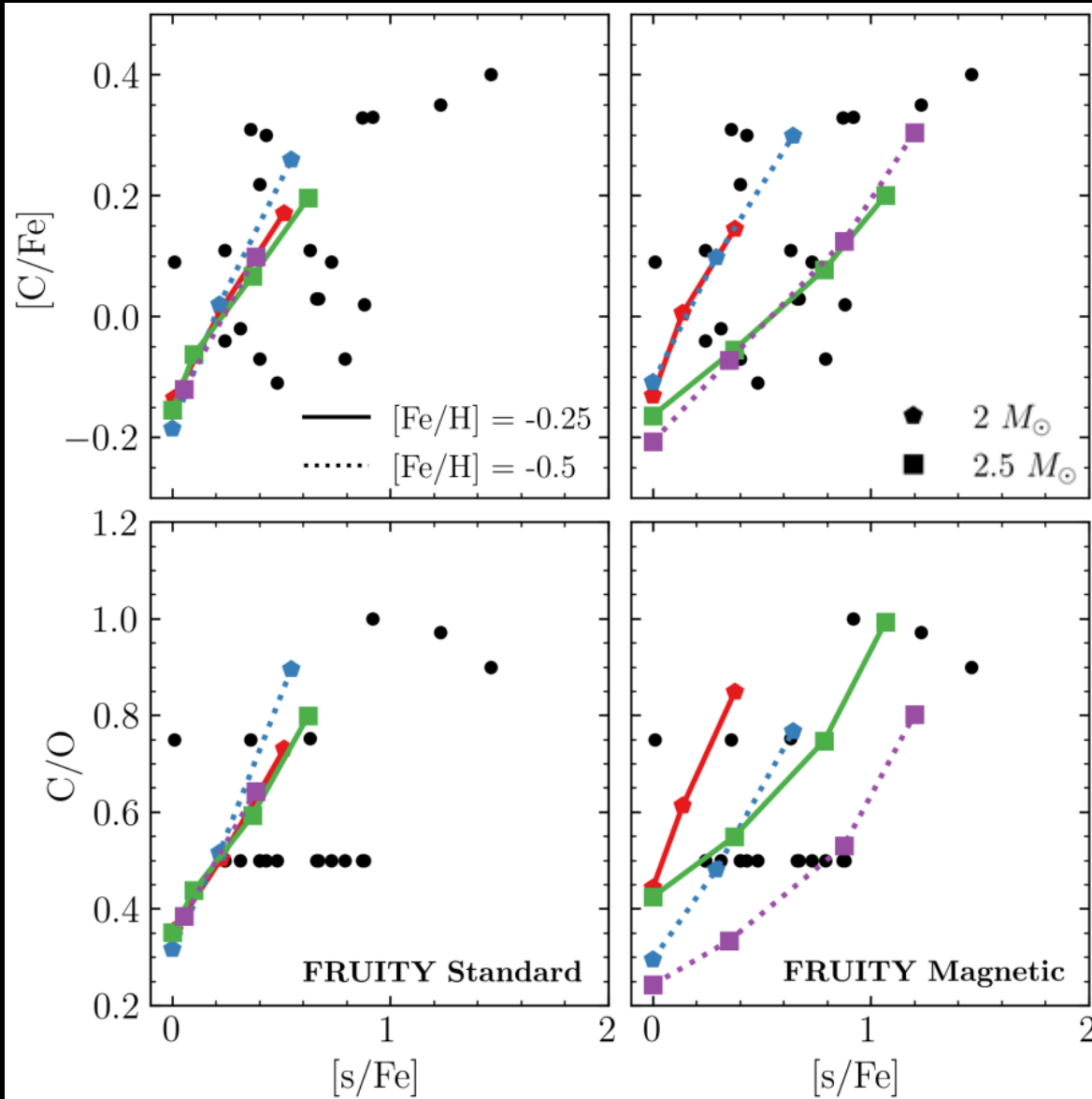


Shetye+18
Shetye+19
Shetye+20
Shetye+21

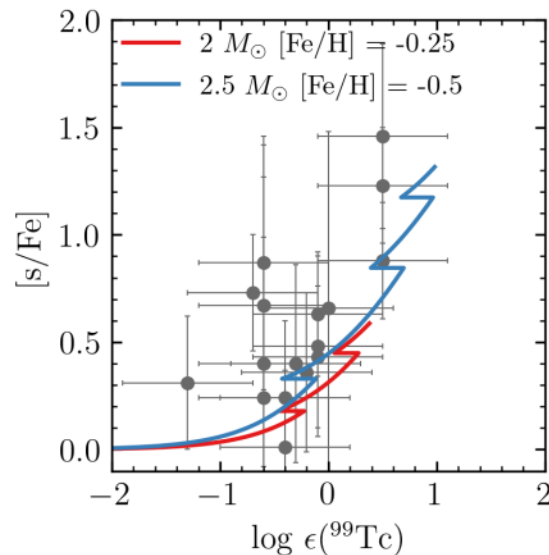
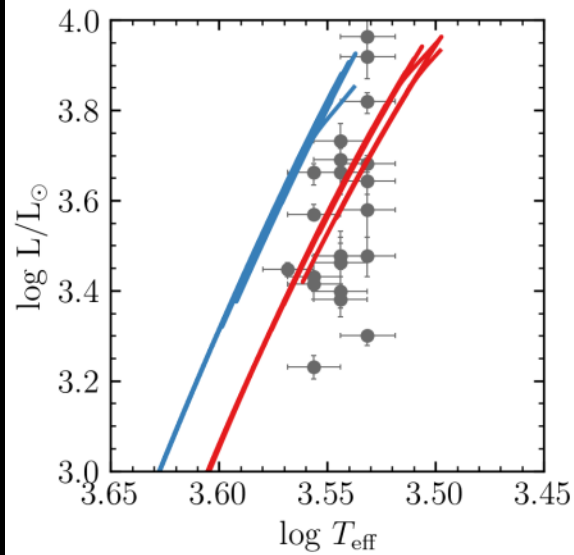
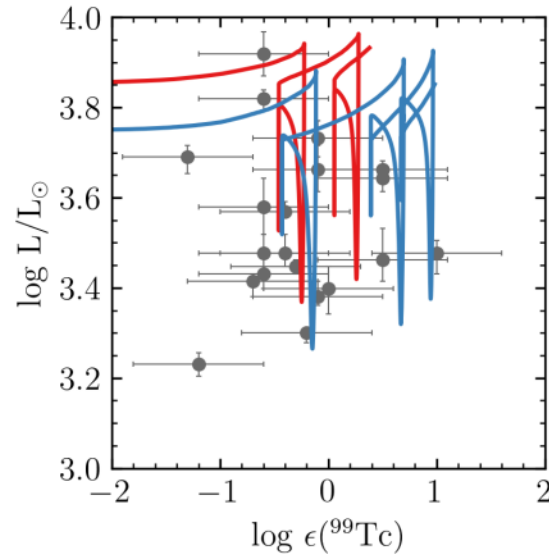
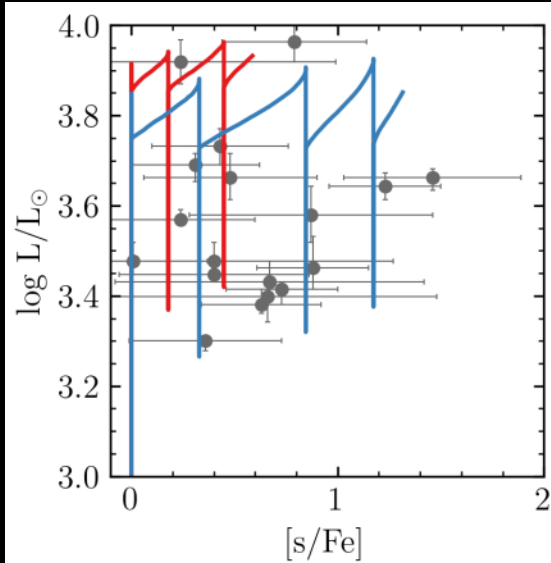


S-stars

$$0.3 < \text{C/O} < 1.0$$

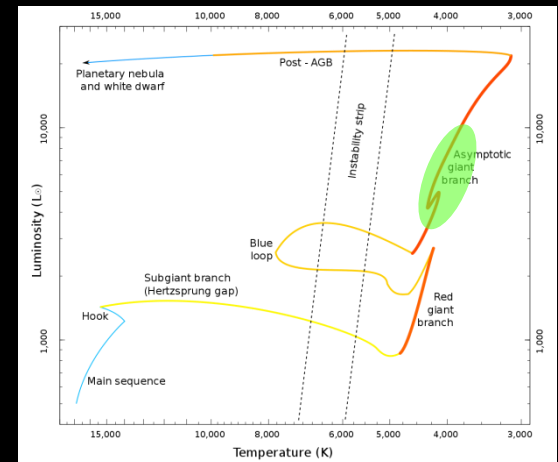


S-stars



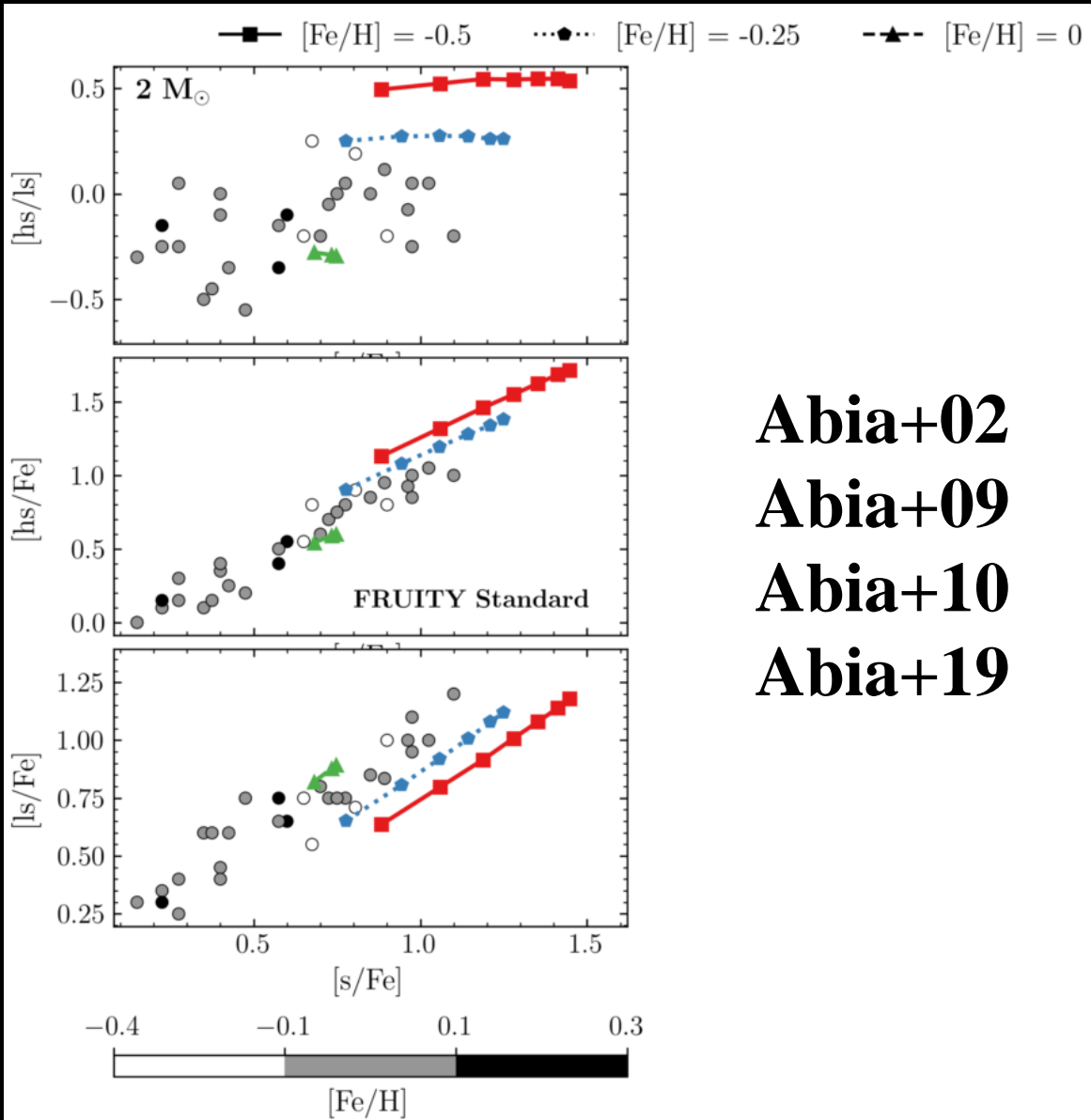
$$0.3 < \text{C/O} < 1.0$$

Tc is freshly produced by TDU [Merrill 1952]

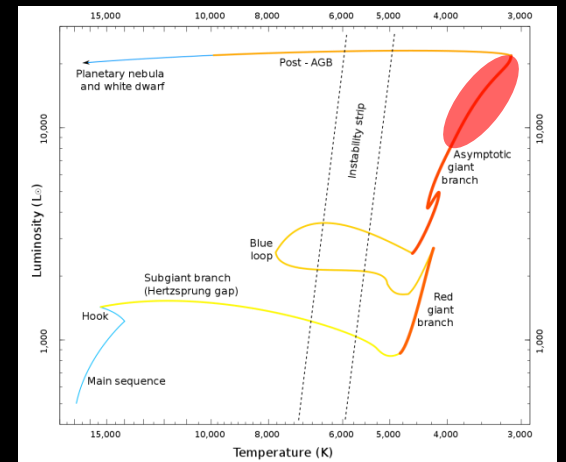


C-stars

$C/O > 1.0$

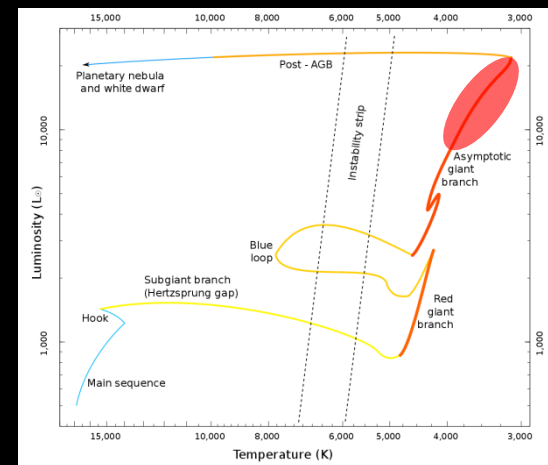
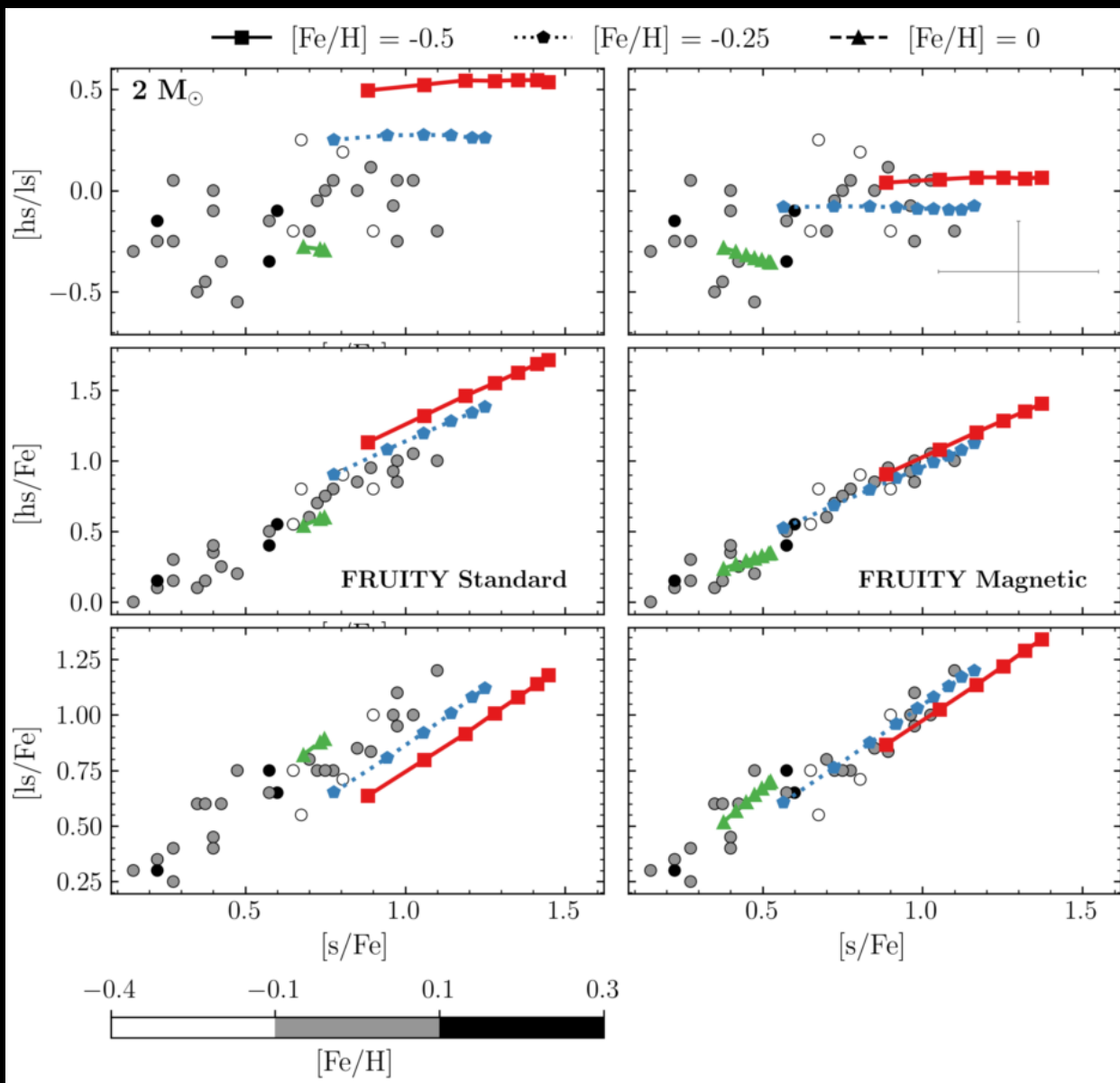


Abia+02
Abia+09
Abia+10
Abia+19

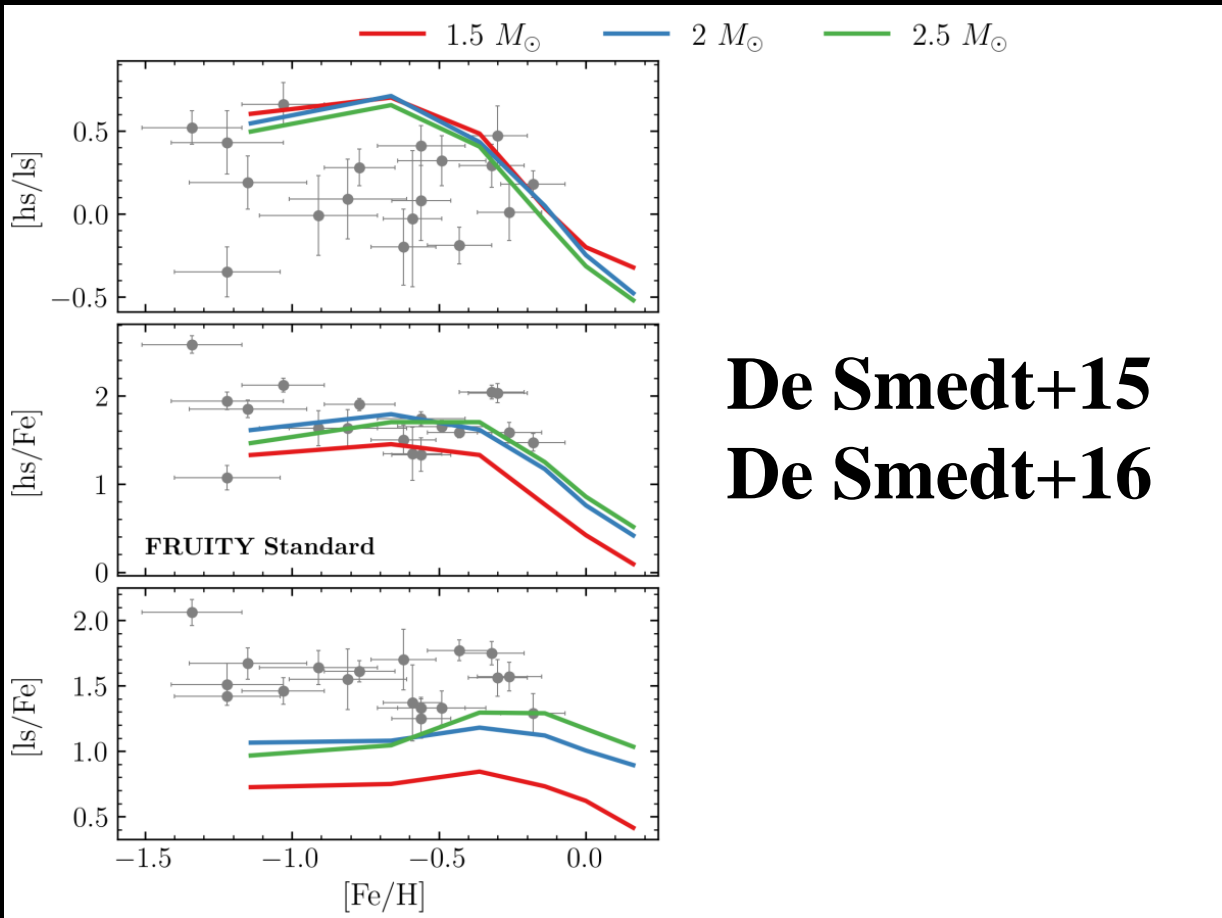


C-stars

$C/O > 1.0$

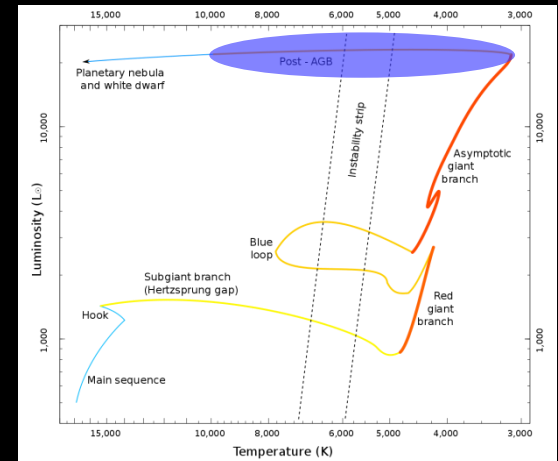


Post-AGB stars

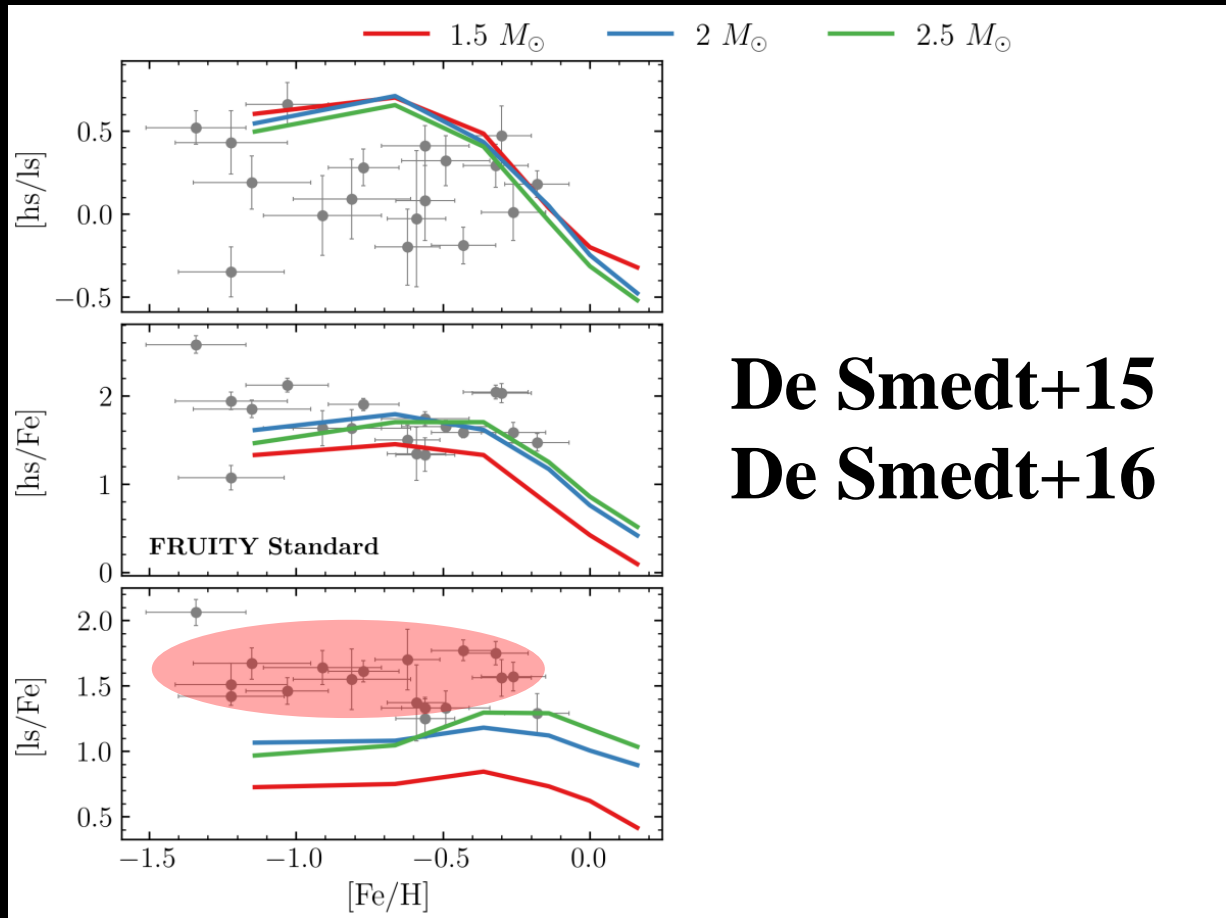


De Smedt+15
De Smedt+16

ls & hs

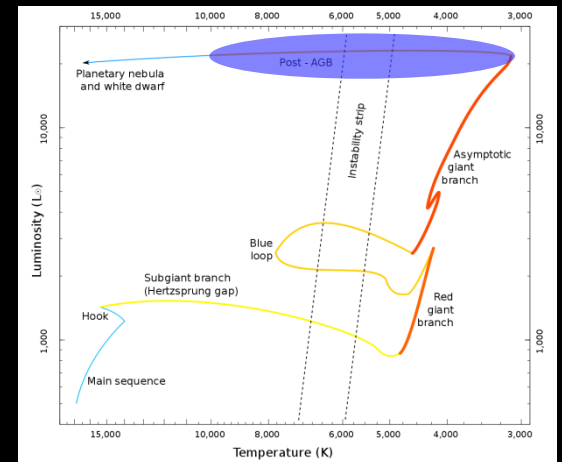


Post-AGB stars

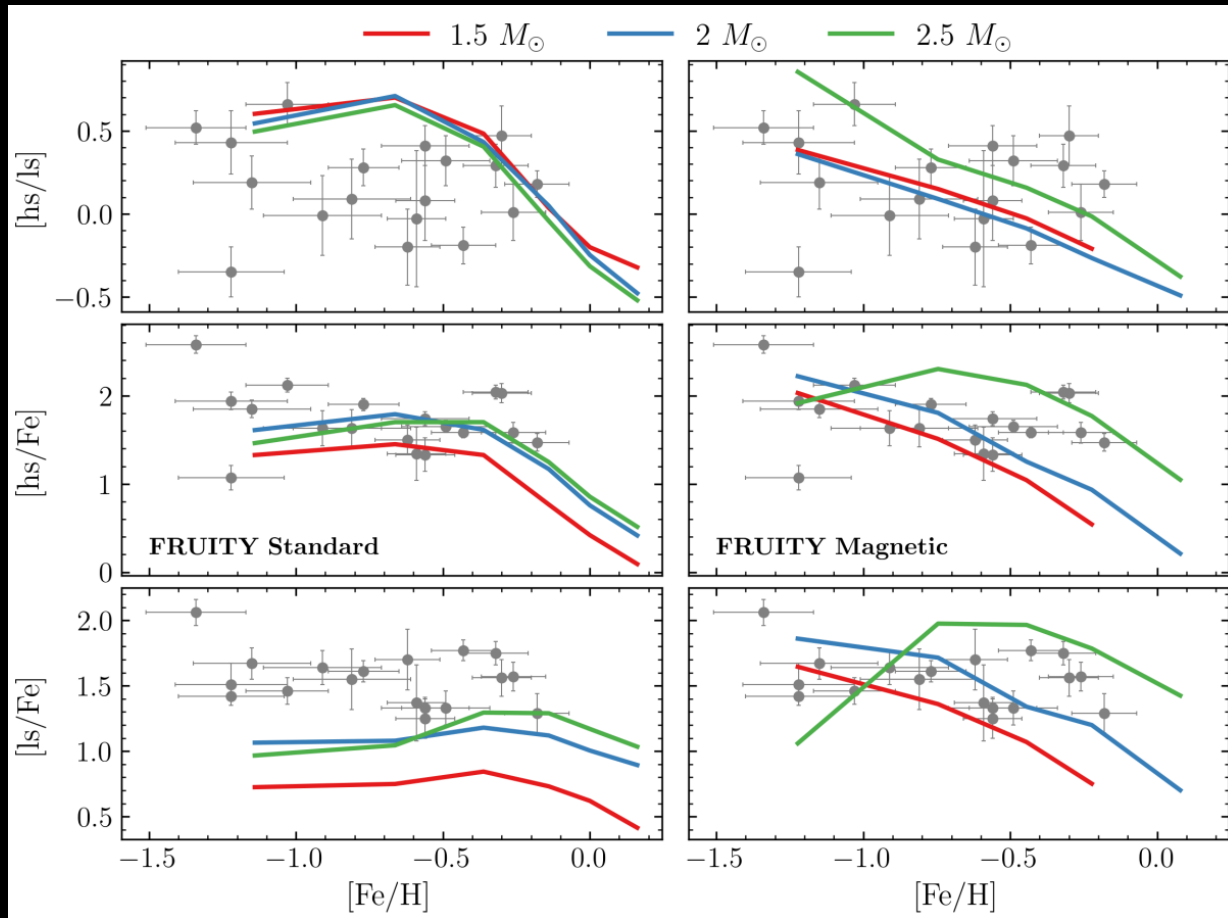


De Smedt+15
De Smedt+16

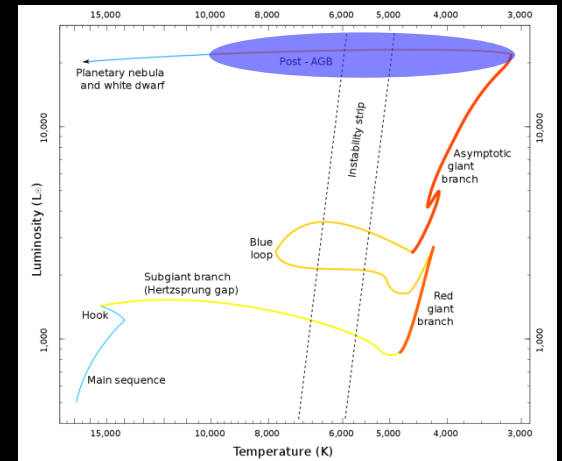
ls & hs



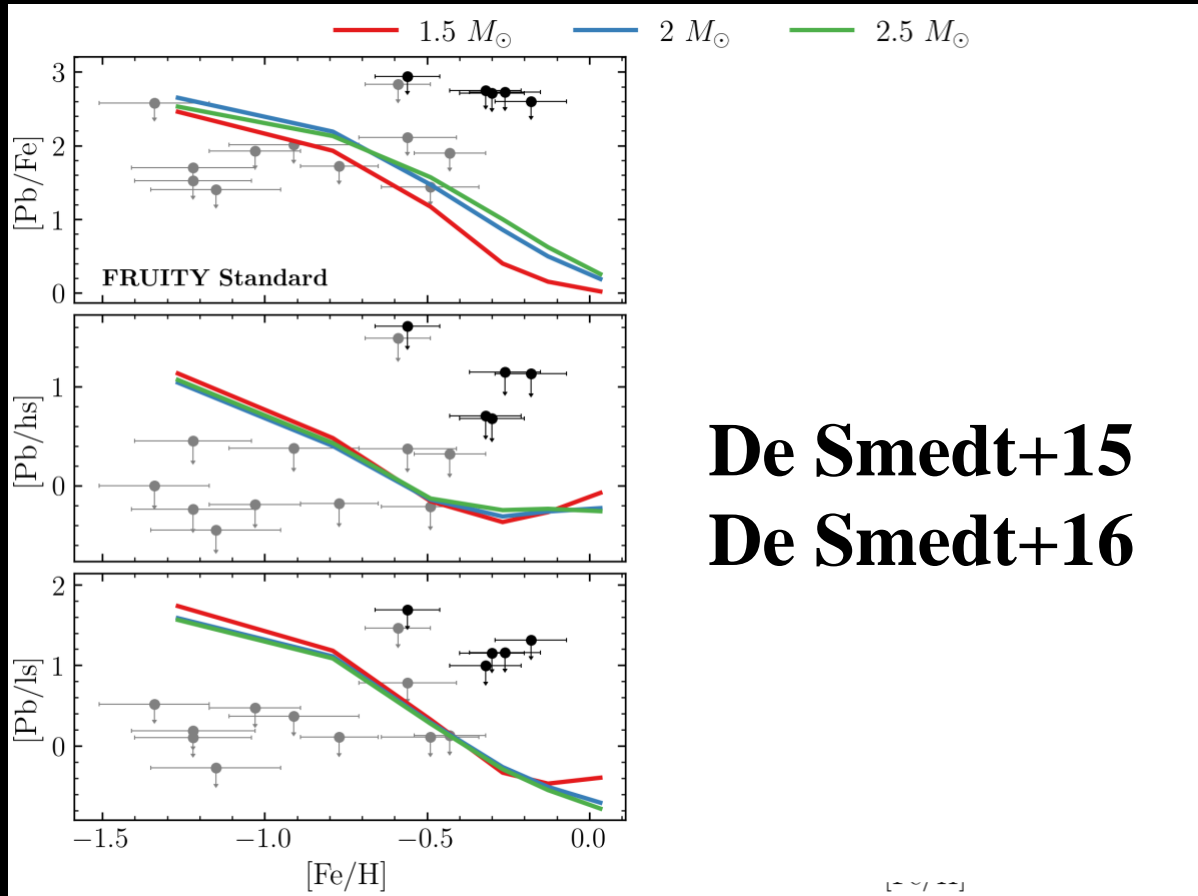
Post-AGB stars



ls & hs

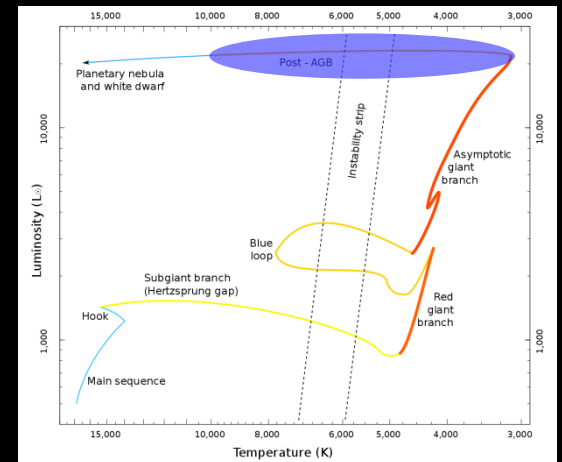


Post-AGB stars

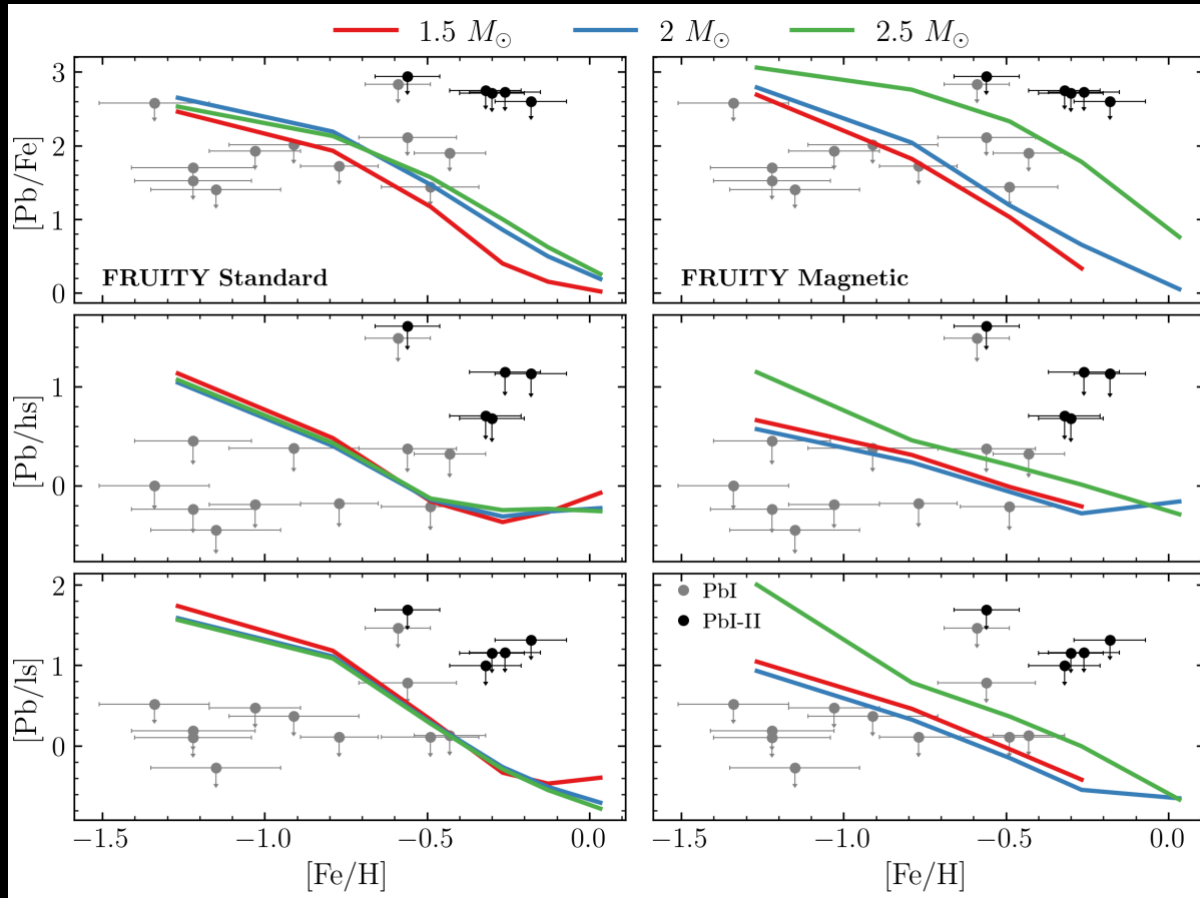


De Smedt+15
De Smedt+16

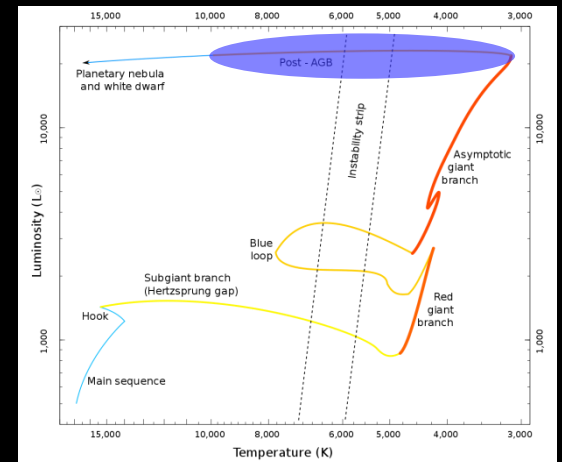
Pb



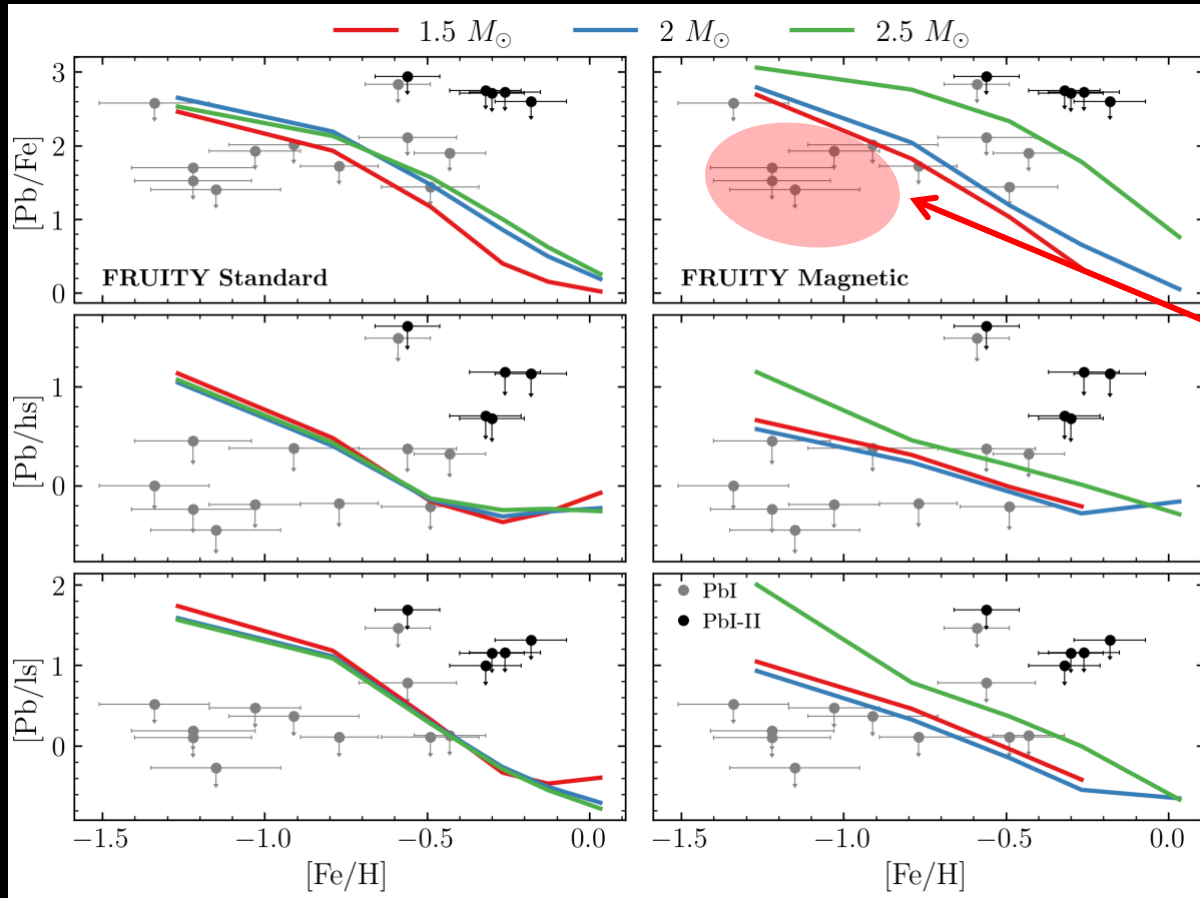
Post-AGB stars



Pb

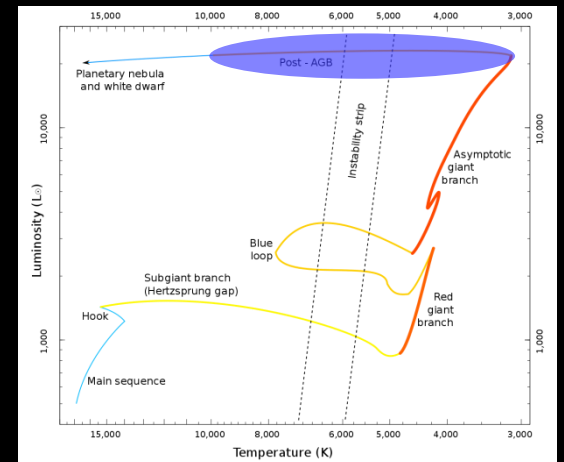


Post-AGB stars

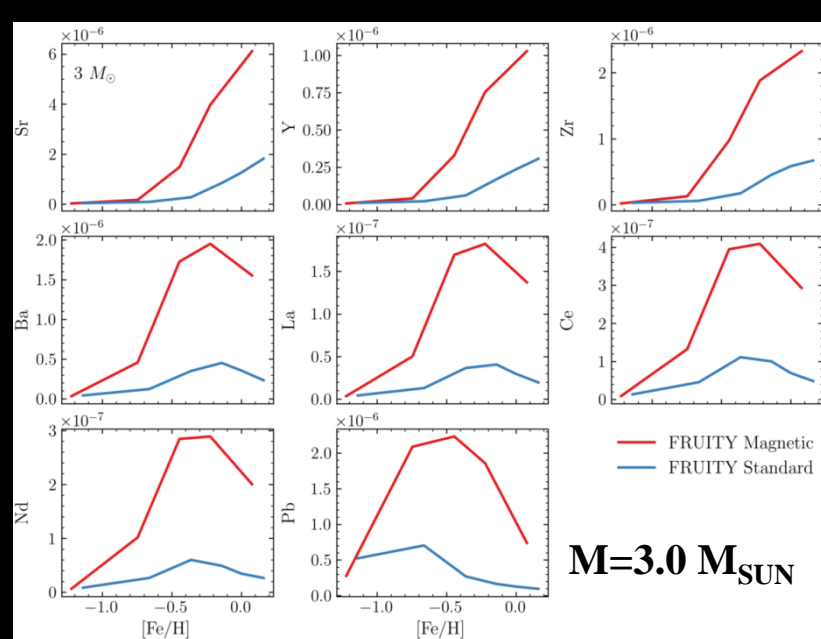
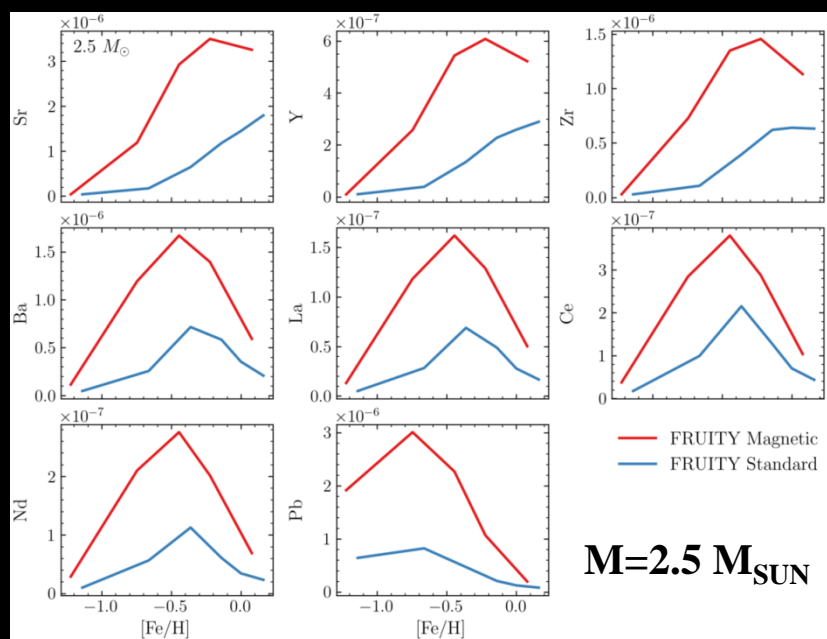
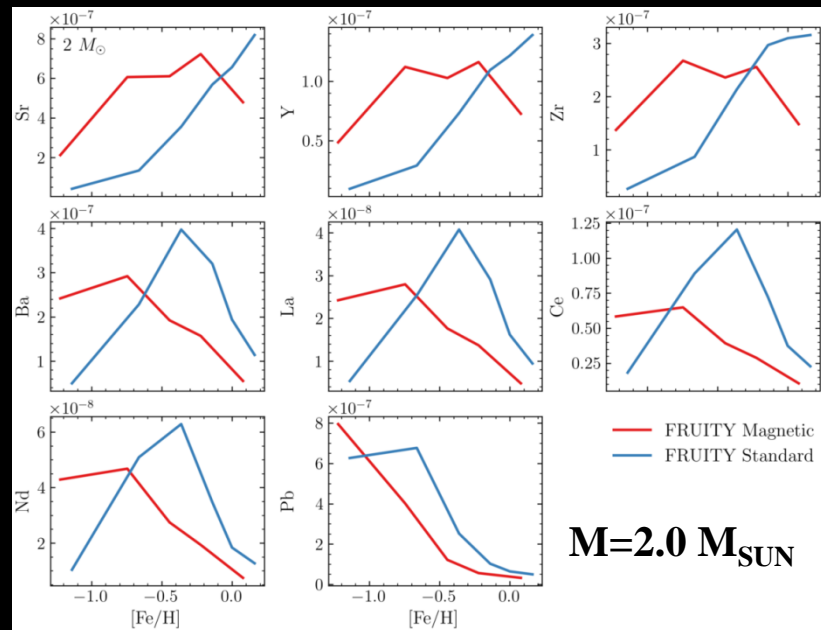
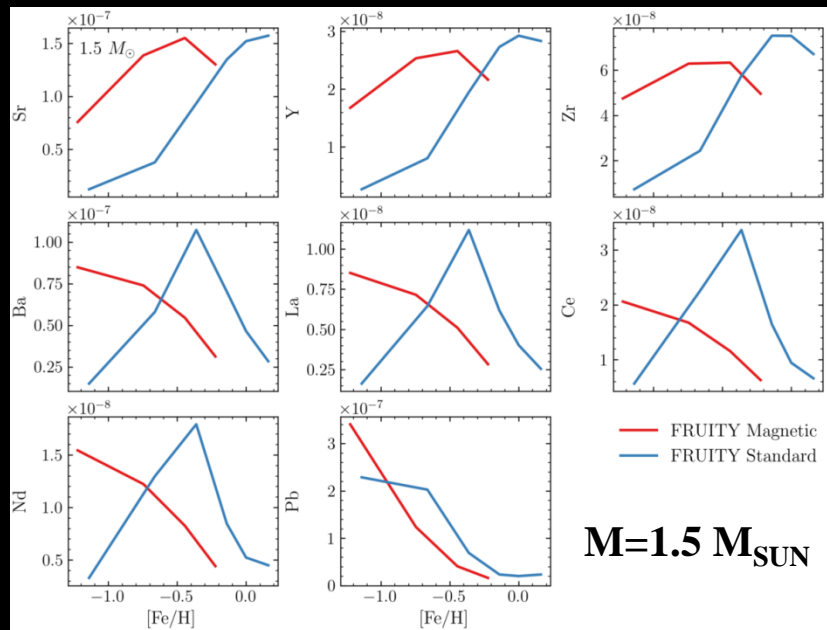


Pb

NLTE effects on Pb I @ low Z?



New Magnetic AGB yields



s, i & r Element Nucleosynthesis (sirEN)

CONFERENCE

Giulianova (Italy), 8-13 June 2025



HOTEL
EUROPA
GIULIANOVA
★★★★



Finanziato
dall'Unione europea
NextGenerationEU



Ministero
dell'Università
e della Ricerca



Italiadomani
PILLOLE REGIONALI
DI SPERANZA E RESILLENZA



INAF
ISTITUTO NAZIONALE
DI ASTRONOMIA

